

**Developed Mechanisms for CROSS-TIER  
and CO-TIER Interference Avoidance in  
FEMTOCELL NETWORKS**

Shahryar Saleem

MEngSc (Telecommunications), MS Computing (Networking)

College of Engineering and Science

Victoria University

SUBMITTED IN FULFILLMENT OF THE REQUIREMENTS

OF THE DEGREE OF

DOCTOR OF PHILOSOPHY

AUGUST 2013

© Copyright by Shahryar Saleem 2013

All Rights Reserved

*To my loving Parents, my lovely wife Nosheen and my beautiful  
daughter Misha*

## DOCTOR OF PHILOSOPHY DECLARATION

I, Shahryar Saleem, declare that the PhD thesis entitled 'Developed Mechanisms for Cross-Tier and Co-Tier Interference Avoidance in Femtocell Networks' is no more than 100,000 words in length including quotes and exclusive of tables, figures, bibliography and reference. This thesis contains no material that has been submitted previously, in whole or in part, for the award of any other academic degree or diploma. Except where otherwise indicated, this thesis is my own work."

---

Shahryar Saleem

Date: August 28, 2013

# Abstract

To deal with the increasing demand of high speed data streaming and good quality voice traffic from mobile users at home, Femtocell Networks are deployed in homes that enables an indoor mobile user to achieve high speed downloading from the internet and make good quality voice calls. A femtocell network also provides relief to an overloaded macrocell network by servicing mobile users at home which without the femtocell network have to be served by the macrocell. However, like all wireless networks, femtocell networks suffer from the problem of interference. In this thesis, a contribution to the existing research on the avoidance of interference in femtocell networks is presented.

In the first part of the thesis, the “cross-tier interference” caused by a femtocell network operating in “closed access mode” to a macrocell user is investigated. Cognitive Radio is implemented in the Femtocell Base Station (FBS). More specifically, a sensing and transmission scheme is presented that allows a cognitive enabled femtocell to actively sense the macrocell spectrum and allocates vacant resources to its

users. In doing so, the cognitive enabled femtocell reduces the amount of interference caused to the macrocell user while using the same shared frequency spectrum. Thus, increasing the macrocell capacity. To increase the cognitive enabled femtocell capacity, a power allocation scheme is used. More specifically, Water-filling power allocation is used. Another scenario of cross-tier interference from femtocells with open access mode is also investigated in the first section of the thesis. A Simple handover strategy between the macrocell and the femtocell is presented to alleviate the problem of cross-tier interference from open access femtocells. In order to deal with the problem of increased number of handovers associated with the open access femtocells, a timer with a minimum and a maximum threshold value is proposed in every macrocell user. The timer makes the macrocell user to wait for a period of time (specified by the minimum and maximum threshold value) and then decide whether to request a handover or not. The proposed timer reduces the number of open access handovers significantly.

In the second part of the thesis, the effect of co-tier interference in both open and closed access femtocells is investigated. A novel femtocell resource allocation scheme is proposed to alleviate the problem of co-tier interference. In the proposed scheme orthogonal resources are allocated to the closed access femtocells to avoid interference to other femtocells while we divide the open access femtocell into two coverage area, inner and an outer coverage area. The resources are allocated to both

coverage areas of the open access femtocells in a way that avoids co-tier interference while also reducing the Resource Block (RB) usage probability which means more RBs are available for femtocell networks.

# Acknowledgements

First of all, I thank Almighty ALLAH for giving me strength and ability to complete this thesis. I would like to thank my supervisor, Dr. Horace King, for his guidance and support during my PhD studies. This dissertation would never have been possible without his belief in my abilities. I admire his dedication, and hard work.

I am thankful to Prof. Michael Faulkner who provided me the initial support with thesis background and guidance early in my candidature. I am also thankful to the administrative staff of School of Engineering and Science (SES), Office of Postgraduate Research and Faculty of Health Engineering and Science, in particular Shukonya Benka, Elizabeth Smith, Melissa Drysdale, Lesley Birch, katie Batterham, kylie Baggetto, Sue Davies, Natalie Gloster and Angela Rojter.

I would like to thank all the past SES and present TEPS students who have encouraged me during this tough time. So a big thank you to Waqas, Micheal, Vandana, Rizwan, Robabeh, Mustafa, Shabbir, Alamgir, Venkat, Rahele, Reza Pourakber, Reza Berangi Hadi, Hojjat, Zaheer, Faizan, Asyik, Hafiza, Sirmayanti, Nithila,

Geordie, Sara and Behaileu. Finally, I would like to thank my family; especially my Father, who encouraged and supported me throughout my PhD, my Mother, who never stopped praying for me, my sisters who believed in me and my Wife who helped me and never complained throughout these 3.5 years.

# Contents

<b>Abstract</b>	<b>v</b>
<b>Acknowledgements</b>	<b>viii</b>
<b>Contents</b>	<b>x</b>
<b>List of Tables</b>	<b>xiii</b>
<b>List of Figures</b>	<b>xiv</b>
<b>List of Abbreviations</b>	<b>xvii</b>
<b>1 Introduction</b>	<b>1</b>
1.0.1 Cross-Tier Interference . . . . .	3
1.0.2 Co-Tier Interference . . . . .	4
1.1 Thesis Contributions and Organisations . . . . .	6
1.2 Related Research Papers . . . . .	8
<b>2 Literature Review</b>	<b>9</b>
2.1 Femtocell Networks . . . . .	9
2.2 Femtocell Access Modes . . . . .	10

2.2.1	Open Access Mode . . . . .	11
2.2.2	Closed Access Mode . . . . .	11
2.2.3	Hybrid Access Mode . . . . .	12
2.3	Relevant Channel Models . . . . .	13
2.3.1	Outdoor Channel Model . . . . .	13
2.3.2	Indoor Channel Model . . . . .	14
2.4	Cross-Tier Interference Avoidance Schemes . . . . .	14
2.4.1	Cognitive Radio Based Cross- Tier Interference Avoidance Approach . . . . .	15
2.4.2	MUE Handover Interference Avoidance Approach . . . . .	22
2.5	Co-tier Interference Avoidance Schemes . . . . .	26
2.6	Summary . . . . .	29
<b>3</b>	<b>Proposed Radio Approach to Avoid Interference from Femtocell to Macro PUE</b>	<b>31</b>
3.1	System Model . . . . .	32
3.1.1	Sensing and transmission scheme for CRFN . . . . .	34
3.1.2	Power Control Schemes . . . . .	35
3.2	System Parameters and Results . . . . .	38
3.2.1	Capacity . . . . .	40
3.2.2	Channel/slot Availability . . . . .	42
3.2.3	Primary User Equipment Outage . . . . .	43
3.3	Summary . . . . .	45
<b>4</b>	<b>Avoidance of Cross-Tier Interference from Open Access Femtocells</b>	

<b>to Macrocell Users</b>	<b>47</b>
4.1 System Model . . . . .	49
4.2 Cross Tier Interference Avoidance from Open Access Femtocells . . .	51
4.2.1 Why Handover? . . . . .	51
4.2.2 Proposed Handover Strategy for Open Access HNB . . . . .	55
4.2.3 Proposed Solution to Minimise Increased Number of Handovers	61
4.3 Simulation Setup . . . . .	63
4.4 Results . . . . .	67
4.5 Summary . . . . .	73
<b>5 Avoidance of Co-tier Interference Between Femtocells With Different Access Modes</b>	<b>75</b>
5.1 System Model . . . . .	77
5.1.1 Channel Models . . . . .	79
5.2 Co-tier interference in an ideal (planned) vs realistic (unplanned) femtocell network . . . . .	80
5.2.1 Path Loss, Lognormal Shadowing and Fast Fading . . . . .	85
5.3 Proposed Scheme to Avoid Co-tier Interference . . . . .	90
5.4 Simulation Parameters . . . . .	95
5.5 Results . . . . .	98
5.6 Summary . . . . .	98
<b>6 Conclusions and Future work</b>	<b>101</b>
6.1 Future Work . . . . .	104
<b>Bibliography</b>	<b>106</b>

# List of Tables

2.1	Open vs Closed access mode . . . . .	12
3.1	Simulation Parameters . . . . .	40
4.1	Simulation Parameters . . . . .	65
4.2	Reduced number of MUE handover requests . . . . .	73
5.1	simulation Parameters and Results . . . . .	95

# List of Figures

1.1	Concept of $T_x$ - $R_x$ Separation . . . . .	2
1.2	UL Cross-tier interference . . . . .	4
1.3	DL Cross-tier interference . . . . .	4
1.4	Co-tier interference . . . . .	5
2.1	Femtocell Architecture . . . . .	11
3.1	System Model consisting of CRFN underlying a GSM network . . . . .	33
3.2	Sensing scheme CRFN . . . . .	34
3.3	Transmission scheme showing C=3 channels, N=8TSs . . . . .	34
3.4	SUE water-filling power allocation . . . . .	36
3.5	SUE feedback to SBS . . . . .	37
3.6	CRFN Capacity: Equal power (solid) and Water-filling (dashed) vs SBS to PBS distance with $\gamma_{th} = \infty$ dB (top), 10dB (middle), 0dB (bottom). . . . .	41
3.7	CRFN Capacity: Zoom of Fig. 3.6. Equal Power and Water-filling vs SBS to PBS distance. . . . .	42
3.8	CRFN channel/slot availability: Equal Power(full) vs Water-filling (dashed) with $\gamma_{th} = \infty$ dB(top), 10dB(middle),0dB(bottom). . . . .	43

3.9	PUE Outage: Equal Power(full) vs Water-filling (dashed) with $\gamma_{th} = \infty$ dB, 10dB, $-\infty$ dB. . . . .	44
4.1	System Model: HNBS employing MNB DL spectrum in TDD manner causes cross-tier interference to MUEs . . . . .	50
4.2	Need for MUE handover as it moves away from MNB . . . . .	52
4.3	MUE Handover Boundries . . . . .	54
4.4	Cross-tier interference avoidance for open access femtocells using Handover . . . . .	58
4.5	Flow chart showing handover processes in MUE and MNB . . . . .	59
4.6	Probability of single and multiple interfering HNBS . . . . .	60
4.7	Simulation snapshot: MUE at the centre of MNB coverage area . . . . .	67
4.8	Simulation snapshot: MUE at the middle of MNB coverage area . . . . .	68
4.9	Simulation snapshot: MUE at the edge of MNB coverage area . . . . .	68
4.10	5 handover requests are sent by MUE as depicted by the black circles. Number of HNBS=100 . . . . .	69
4.11	13 handover requests are sent by MUE as depicted by the black circles. Number of HNBS=500 . . . . .	69
4.12	16 handover requests are sent by the MUE as depicted by the black circles. Number of HNBS=1000 . . . . .	70
4.13	Reduced number of handovers after 10 and 30 msec timer for 100 HNBS	71
4.14	Reduced number of handovers after 10 and 30 msec timer. Purple circles show where a handover is necessary. Number of HNBS=500 . . . . .	71
4.15	Reduced number of handovers after 10 and 30 msec timer. Purple circles show where a handover is necessary. Number of HNBS=1000 . . . . .	72

5.1	System Model . . . . .	77
5.2	Ideal femtocells configuration . . . . .	81
5.3	Interfering $HNB_1$ to victim $HUE_0$ distance calculation . . . . .	82
5.4	Interference due to planned femtocell configuration . . . . .	82
5.5	Unplanned femtocell configuration . . . . .	83
5.6	Interference due to unplanned femtocell configuration . . . . .	83
5.7	RoI with only Path loss . . . . .	85
5.8	Interference due to unplanned femtocell configuration including shadowing and fast fading . . . . .	87
5.9	RoI with only Path loss, shadowing and Rayleigh fading . . . . .	88
5.10	Region of Interference versus the HNB coverage area . . . . .	88
5.11	Probability of $HUE_0$ interference from a single interfering HNB . . . . .	89
5.12	Probability of $HUE_0$ interference from multiple interfering HNBs . . . . .	90
5.13	Proposed solution incorporating a FNC inside the macrocell . . . . .	91
5.14	Proposed RB allocation scheme . . . . .	93
5.15	RB allocation to open and closed access HNBs . . . . .	94
5.16	Snapshot of $HUE_0$ near $HNB_0$ . . . . .	96
5.17	Snapshot of $HUE_0$ at the coverage edge of $HNB_0$ . . . . .	97
5.18	Avoidance of interference to $HUE_0$ from our proposed resource allocation scheme . . . . .	99

# List of Abbreviations

AHM	Adaptive Hysteresis Margin
AI	Available Intervals
CRFN	Cognitive Radio Femtocell Network
CR	Cognitive Radio
CFBS	Cognitive Radio Femtocell Base Station
CFCA	Combination of Frequency bandwidth dynamic division and Clustering Algorithm
CRRM	Cognitive Radio Resource Management
CP	Critical Places
CAC	Call Admission Control
CINR	Carrier to Interference and Noise Ratio
CC	Component Carrier
CSI	Channel State Information
CN	Core Network
DL	Downlink
DSL	Digital Subscriber Line
DLMAP	Downlink Medium Access Protocol
eNB	Evolved Node B

FBS	Femtocell Base Station
FDD	Frequency Division Duplex
FSC	Femtocell System Controller
FNC	Femtocell Network Controller
FDMA	Frequency Division Multiple Access
GSM	Global System for Mobile Communication
GPS	Global Positioning System
HNB	Home Node B
HUE	Home User Equipment
HeNB	Home Evolved Node B
HM	Hysteresis Margin
HDT	Handover Delay Timer
IWF	Iterative Water-filling
LTE	Long Term Evolution
LTE-A	Long Term Evolution Advanced
LDO	Low Duty Operation
MNB	Macro Node B
MBS	Macrocell Base Station
MUE	Macrocell User Equipment
OFDMA	orthogonal Frequency Divison Multiple Access
PBS	Primay Base Station
PUE	Primary User Equipment
PCC	Primary Component Carrier
PDCCH	Physical Downlink Common Control Chaneel

QoS	Quality of Service
RSS	Received Signal Strength
RB	Resource Block
$R_x$	Receiver
REM	Radio Environment Map
RSSI	Received Signal Strength Indicator
RBUR	Resource Block Usage Report
SBS	Secondary Base Station
SUE	Secondary User Equipment
SIR	Signal to Interference Ratio
SCC	Secondary Component Carrier
SQ	Service Quality
$T_x$	Transmitter
3GPP	Third Generation Project Partnership
TDD	Time Division Duplex
TDMA	Time Division Multiple Access
TS	Time Slot
UL	Uplink
UE	User Equipment
UMTS	Universal Mobile Telecommunication System
UAI	Unavailable Intervals
X2	Interface allowing to interconnect eNBs with each other

# Chapter 1

## Introduction

In recent years there has been an exponential growth of wireless communication services and more and more mobile users use wireless services indoors. Studies conducted on the usage of wireless networks report that more than 50% of voice and more than 70% of data traffic originate from users located indoors [1]. The indoor users require (a) high signal level from the Macrocell Base Station (MBS) to accomplish good quality voice calls, and enjoy high speed downloading from the internet. However, as the MBS may be mounted far away from user's premises, thus it may not be possible that the signal level quality from the MBS to the indoor user is very good to support good voice and data traffic. Thus, there is a need to provide high capacity wireless links indoors that can provide high signal quality to the indoor user to achieve excellent voice communications and support high speed data traffic. This high link capacity can be achieved by bringing the transmitter ( $T_x$ ) and the receiver ( $R_x$ ) closer to each other. Illustration of concept of  $T_x$ - $R_x$  separation is shown in Figure 1.1. It is evident from Figure 1.1 that due to larger  $T_x$ - $R_x$  separation the signal level quality at the user's home is very low (the communication link is shown in red color to depict the

poor signal level quality). Due to the large  $T_x-R_x$  separation, the wireless channel parameters such as path loss and fast fading degrades the signal from transmitter to the receiver. On the other hand, smaller  $T_x-R_x$  separation promises high signal level quality (as shown by the green color of the communication link).

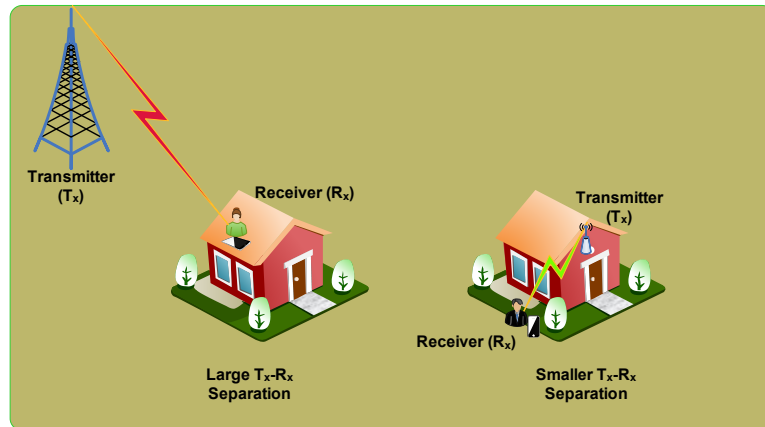


Figure 1.1: Concept of  $T_x-R_x$  Separation

Femtocell Networks [1] [2] and [3] exploit this reduction in  $T_x-R_x$  separation to provide high quality wireless links and good spatial usage [1]. There are two common spectrum access approaches for femtocell deployment. 1. Dedicated channel access [4] and [5] and 2. Co-channel access. In dedicated channel access approach, the entire available spectrum is divided into several frequency bands and femtocell use different frequency bands than the macrocell. Thus, avoiding cross-tier interference completely. However, this approach is limited due to the fact that a large number of femtocell deployments can occur inside a macrocell and thus each femtocell only utilises a very limited bandwidth. Another partial co-channel access scheme is proposed in [6], where the MBS divides the available frequency spectrum into a macrocell dedicated part and a femtocell/macrocell shared part. The MBS puts those Macrocell User Equipment (MUE) into the dedicated part which causes interference to femtocells. This approach

seems to increase the spectrum reuse but the scheme becomes inefficient if the number of MUEs near the femtocell increase. Thus, a practical solution is the co-channel access where femtocell and macrocell share the same available spectrum. In this thesis the co-channel spectrum access is adopted by the femtocells to improve the spectrum reuse efficiency. However, due to the fact that femtocells inside the macrocell use the same macrocell spectrum for communication, the probability that a femtocell will cause interference to a macrocell is significantly high. Similarly, the probability that a macrocell will cause interference to a femtocell is also very high. In addition, the probability that a femtocell will cause interference to another femtocell is also very high. The above mentioned femto-macro and femto-femto interference types are Cross-tier interference (femto-macro or macro-femto) and Co-tier interference (femto-femto) [2], [7], [8], [9] and [10]. An explanation of both these interference types are given below along with the interference scenarios for both Uplink (UL) and Downlink (DL). In this thesis the terminologies from the Third Generation Partnership Project (3GPP) will be used to denote femtocell entities and macrocell entities [3]. In 3GPP terms, a FBS is known as a Home Node B (HNB) and a femtocell user is known as a Home User Equipment (HUE). Similarly, the MBS in 3GPP terminology is known as Macro Node B (MNB) and the macrocell user is known as the MUE [11] and [12].

### 1.0.1 Cross-Tier Interference

Cross-tier interference as the name implies is between entities that belong to different tiers or networks. Such interference exists between femto-macro and macro-femto. In the UL direction, a MUE near a HNB and away from its MNB transmitting in the UL direction at high power will drown the UL signal from the HUE to its HNB, or a

HUE near the MNB can drown the UL signal from a far away MUE transmitting to its MNB. Both scenarios for UL interference are shown in Figure 1.2

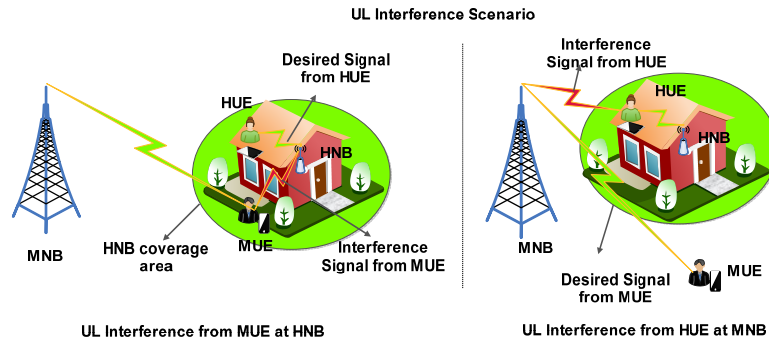


Figure 1.2: UL Cross-tier interference

In the DL direction, a MNB transmitting at high power to its far away MUE will drown the DL signal from HNB to its HUE. Similarly, a MUE near a HNB and far away from its MNB will be interfered in the DL direction by the HNB. Both scenarios for DL interference are shown in Figure 1.3.

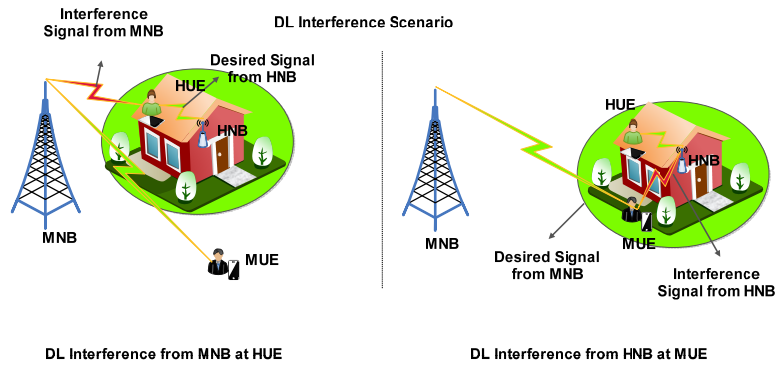


Figure 1.3: DL Cross-tier interference

## 1.0.2 Co-Tier Interference

Co-tier interference is the interference between entities that belong to the same tier or network. In case of a femtocell network, the co-tier interference occurs between

neighbouring femtocells. In the UL direction, a HUE (aggressor) causes interference to the nearby HNB. In the DL direction, a HNB causes interference to the nearby HUEs belonging to different femtocell networks. Co-tier interference scenario is depicted in Figure 1.4.

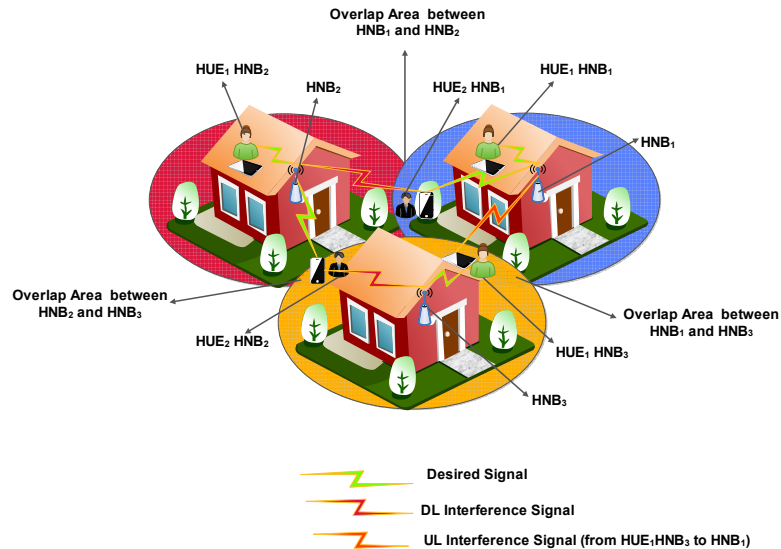


Figure 1.4: Co-tier interference

The above mentioned interference types have severe impacts on the performance of the femtocell network as well as the macrocell network. Due to these interferences the advantage of high capacity wireless links diminishes. Thus, in order to extract the most out of the femtocell network, schemes are necessary to avoid the cross-tier and co-tier interferences. The avoidance of femto-macro and femto-femto interference where femtocells operate in co-channel access mode is the main focus of this thesis.

## 1.1 Thesis Contributions and Organisations

The motivation behind this research is highlighted in the previous section. In this thesis novel schemes are proposed to avoid cross-tier and co-tier interferences. This thesis makes a contribution to the existing body of literature on the avoidance of cross-tier and co-tier interference. This thesis consists of 6 parts and each part is compiled as a chapter. Below, we give a brief outline of work done in each chapter.

- Chapter 2 provides the necessary background information that will be used in this thesis. A relevant summary of literature on cross-tier and co-tier interference mitigation schemes is provided in this chapter.
- Chapter 3 is the first technical part of the thesis. In this chapter a sensing and access scheme which enables the Time Division Duplex (TDD) operation of an underlay Cognitive Radio Femtocell Network (CRFN) in a Frequency Division Duplex (FDD) macrocell is proposed. The sensing scheme avoids the cross-tier interference from FBS to the MUE and the access scheme increases the capacity of the femtocell network. The outage performance of the macro cell (the primary system) and the capacity performance of the CRFN (the secondary system) as a function of the MBS to FBS separation is studied. In addition, we also consider the effect of multichannel operation of the CRFN for increased throughput. Further improvements are obtained by water-filling the transmit power across the channels
- In Chapter 4, schemes to avoid cross-tier interference from open access femtocells to MUE inside a macrocell are proposed. Cross-tier interference is avoided by allowing macrocell users to handover to the interfering femtocell. However,

the MBS can only use those femtocell resources which are un-utilised and have very low level of interference from the macrocell. In order to deal with the problem of increased number of handovers associated with the open access femtocell, a timer is proposed in every macrocell user. The timer helps to correctly identify the need for a handover. This way the unnecessary requests for handover by the macrocell user are reduced

- In Chapter 5, the focus of the thesis turns towards the effect of co-tier interference and in this chapter a novel resource allocation based scheme that avoids co-tier interference from femtocells with different access modes is proposed. In particular, we propose a femtocell network controller (FNC) connected to a large density of femtocells. The FNC acts as a “virtual” macro- base station for the core network (CN) and as a “virtual” CN entity for the HNBs. The FNC is responsible for allocating resources to all HNBs that are connected to it. Furthermore, we also propose that orthogonal resources are allocate to the closed access femtocells while we divide the coverage area of the open access femtocells into two separate coverage areas, inner coverage area and outer coverage area. The inner coverage area is allocated resources that are used by the nearest closed access femtocell while the outer coverage area is allocated resources that are used by the far away closed access femtocells. This resource allocation avoids the co-tier interference in the dense femtocell network while the scheme also reduces the RB usage probability.
- Chapter 6 concludes the work in this thesis and also recommends future research work. This includes the research on avoiding cross-tier and co-tier interference in the UL direction.

## 1.2 Related Research Papers

This research work has led to the following contributions to the existing literature.

1. S. Saleem, H. King, "Avoidance of Cross-tier Interference from Open Access Femtocells to Macrocell Users," *Journal of Communication and Computer (JCC)*, pp. 929-941, vol. 9, no. 8, Aug. 2012.
2. S. Saleem, H. King, "Avoidance of Co-tier Interference between Femtocells with Different Access Modes," *International Journal of Information and Communication Technology Research (IJICTR)*, pp. 617-626, vol. 2, no. 8, Aug. 2012.
3. S. Saleem, W. Ahmed, "Transmission in Black Space, A Paradigm in Cognitive Radio Networks," Presented by S. Saleem at ARC Cognitive and Multi-hop Wireless Networking Workshop, 2010.[Online]: <http://www.acorn.net.au/event/mwnworkshop10/>
4. R. Berangi, S. Saleem, M. Faulkner and W. Ahmed, "TDD Cognitive Radio Femtocell Network (CRFN) Operation in FDD Downlink Spectrum," in *Proceedings Personal Indoor and Mobile Radio Communications (PIMRC)*, pp. 482-486, 11-14 Sept. 2011.
5. W. Ahmed, J. Gao, S. Saleem and M. Faulkner, "An Access Technique for Secondary Network in Downlink Channels," in *Proceedings Personal Indoor and Mobile Radio Communications (PIMRC)*, pp. 423-427, 11-14 Sept. 2011.
6. Co-tier Interference Avoidance between Femtocells Using Cell Sectoring, currently being drafted for submission to a journal.

# Chapter 2

## Literature Review

The main aim of this chapter is to provide an overview on the most recent developments to rectify cross-tier and co-tier interference in femtocell networks. In Section 2.1 the main architecture of the femtocell network is discussed. In Section 2.2, three femtocell access modes are discussed. This is followed by a review of cross-tier interference avoidance schemes in Section 2.4. In Section 2.5, a literature review of the schemes that avoid co-tier interference is presented.

### 2.1 Femtocell Networks

Femtocell Networks are the promising solution to provide high wireless link capacity. A Femtocell network consists of a Femtocell Base Station and a Femtocell user. The HNB communicates with the HUEs that are present indoors and provide excellent voice and data traffic experience. The main benefits of femtocell networks are;

- Easy installation. Just plug the femtocell into the DSL or cable modem. No configuration is required by the home user.

- Seamless handover. Mobile phones associated with the femtocell automatically switch to the femtocell from the macrocell upon arrival into their homes.
- Excellent voice quality at home.
- High data rates for fast streaming and downloads by the indoor user.
- Increased mobile phone battery life. The mobile phone associated with a femtocell experience increase in battery life as compared to when connected to the macrocell.

The femtocell is connected to the service provider network through optical cables or high speed Digital Subscriber Line (DSL) [2]. The femtocell operates in *co-channel* mode meaning that the femtocell and the macrocell shares the same frequency spectrum. This co-channel operation increases the spectrum utilisation. Because the femtocells allow indoor users to communicate with the macrocell network through itself, the femtocell eases the traffic load on the macrocell which increases the macrocell capacity. The femtocell architecture is shown in Figure 2.1 [2].

## 2.2 Femtocell Access Modes

In this section we discuss the modes by which a femtocell can be accessed. A femtocell can operate in one of the three access modes namely open access mode, closed access mode and hybrid access mode. A brief description of each of these modes is given below.

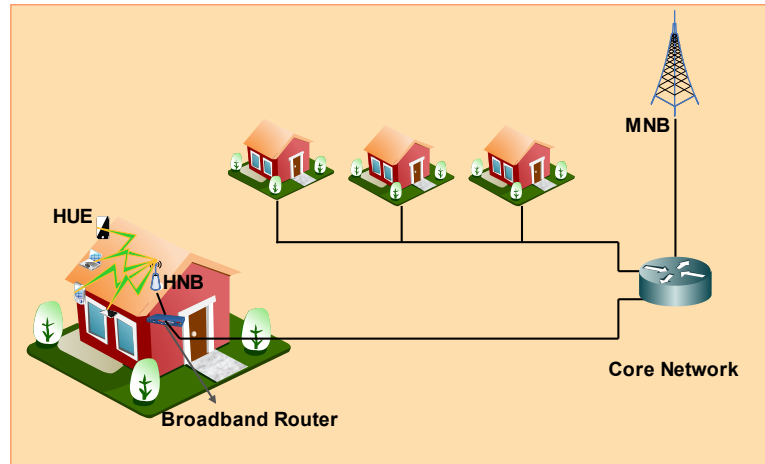


Figure 2.1: Femtocell Architecture

### 2.2.1 Open Access Mode

If a femtocell has *Open Access* mode [8] and [13], all mobile users (registered or unregistered) can access that femtocell. Thus every mobile user is always connected to the femtocell that provides the best signal quality. The open access femtocells are mostly deployed in shopping malls and office buildings where all mobile users can communicate with that femtocell. The challenges of open access femtocell deployments are increased handovers between open access femtocells and between open access femtocells and the macrocell [8]. In this thesis, a solution is proposed that reduces the number of unnecessary handovers between caused due to the deployment of the open access femtocells.

### 2.2.2 Closed Access Mode

In contrast to the open access mode, If a femtocell operates in *Closed Access* mode [8] and [13], only registered users are served by that femtocell. If the unregistered or non associated user is closer to the closed access femtocell than the macrocell base station,

Table 2.1: Open vs Closed access mode

Open access femtocells	Closed access femtocells
More handovers	Higher interference
Higher network throughput	Lower network throughput
Increased outdoor capacity	Serves only indoor users
Shopping malls, offices	Home market
Security issues	Easier billing

and the femtocell base station is able to provide the best signal quality to the non associated user even then, the non associated user will not be allowed to connect to the closed access femtocell. The closed access mode along with co-channel access creates the most severe of interference between femto-macro and femto-femto. These types of femtocells are mainly deployed by private owners. The main characteristics of both open and closed access modes are given in Table 2.1.

### 2.2.3 Hybrid Access Mode

In a hybrid access mode, a femtocell operates in open access mode and closed access mode at the same time. The hybrid access femtocell does not only provide service to registered users but also serve the unregistered users. However, the unregistered users are given a limited Quality of Service (QoS) and low priority when registered users are also in the vicinity of the hybrid access femtocell [14]. In this thesis, only open access and closed access modes in femtocells are investigated.

## 2.3 Relevant Channel Models

In this section the relevant channel models for the communication paths from the macrocell base station to the macrocell user equipments and the femtocell user equipments are discussed.

### 2.3.1 Outdoor Channel Model

Chapter 3 and Chapter 4, use the COST-231 Walfisch Ikegami [15], [16] and [17] path loss model for paths between PBS and PUEs, PBS and Cognitive Radio Femtocell Network (CRFN) and between PUEs and CRFN in Chapter 3. In Chapter 4, the same model is used for the paths between the MNB and the MUE and between the MNB to HNB. In our models we assume a non line of sight (NLOS) between  $T_x$  and  $R_x$ , thus the expression for path loss for NLOS condition is expressed as:

$$P_L(dB) = P_{L0} + L_{rts} + L_{msd} \quad (2.1)$$

Where:

$$P_{L0}(dB) = 32.4 + 20 \log_{10}(d) + 20 \log_{10}(f_c) \quad (2.2)$$

$$L_{rts} = -16.9 - 10 \log_{10}(w) + 10 \log_{10}(f_c) +$$

$$20 \log_{10}(\Delta h_m) + L_{ori}, \text{ and}$$

$$L_{msd} = L_{bsh} + k_a + k_d \log_{10}(d) + k_f \log_{10}(f_c) - 9 \log_{10}(b)$$

$L_{rts}$  is the rooftop-to-street diffraction and scatter loss,  $L_{ori}$  is the orientation loss and  $L_{msd}$  is the multiple screen loss.  $L_{bsh} = -18 \log_{10}(1 + \Delta h_b)$ ,  $d$  is the distance in

km and the carrier frequency  $f_c$  is in MHz. We take  $K_a = 54$  which is the path loss coefficient for base station antennas below rooftops of adjacent buildings,  $K_d = 18$  and  $K_f = -4 + 1.5(\frac{f_c}{925} - 1)$  are the multiscreen diffraction loss versus distance and radius and frequency for metropolitan areas. The antenna heights are 11m for the base station, 1.5m for the mobiles and the roof heights are 10m, with the buildings on a  $w = 50\text{m}$  pitch.

### 2.3.2 Indoor Channel Model

For indoor propagation effects we employed the IEEE 802.11n channel model D (typical office) in Chapter 3. The break point distance is 10m where the path loss exponent increases from 2 to 3.5. This gives us a free space path loss model expressed below as;

$$P_L dB = 35 \log_{10}\left(\frac{d}{0.01}\right) + 20 \log_{10}(0.01) + 20 \log_{10}(f) + 32.45 \quad (2.3)$$

In addition to the path loss models described above we have also included fading and shadowing in the transmission paths. For the macrocell fading we assume Rayleigh fading and for indoor fading we assume Rician fading ( $K=10\text{dB}$ ). Outdoor and indoor shadowing was also considered to obtain realistic results as highlighted in [18].

## 2.4 Cross-Tier Interference Avoidance Schemes

In this section, a review of the schemes to avoid cross-tier interference is presented. The performance of the schemes and their drawbacks which led to this research are

also discussed.

### 2.4.1 Cognitive Radio Based Cross- Tier Interference Avoidance Approach

Cognitive Radio (CR) [19] was proposed to minimise the underutilisation of the frequency spectrum [20] and [21]. In CR terms, the cognitive enabled femtocell base station is often termed as a Secondary Base Station (SBS), the user accessing the SBS is termed as Secondary User Equipment (SUE). The macrocell base station is termed as Primary Base Station (PBS) and its user is termed as Primary User Equipment (PUE). A CR empowered femtocell is a femtocell that can sense the macrocell frequency spectrum, look for spectrum holes [22] (unused macrocell frequency spectrum) and adapt its transmission power to transmit in the spectrum holes causing no interference to the macrocell PUE [23]. Thus, increasing the spectrum utilisation of the macrocell (primary) spectrum. The three well known secondary spectrum allocation approaches are *Interweave*: sense and transmit in *Spectrum Holes* [22], *Overlay*: sense and transmit on the same channel, and *Underlay*: transmit parallel to the primary transmissions under a specified interference threshold level [24]. As discussed above, a cognitive femtocell increases the capacity of the macrocell and avoids PUE outage by opportunistically using the frequency spectrum. However, the capacity in terms of Bits/s/Hz of a femtocell is also of great importance. Hence, along with sensing scheme to reduce the outage to the PUE, a transmission scheme must also be used in a cognitive femtocell that enables high capacity links between SBS to SUE and vice versa. In the following a relevant literature review on sensing and transmission schemes is presented below. A combination of CR and a conventional femtocell was

proposed by [13]. In the paper, the authors proposed a Cognitive Radio Femtocell Base Station (CFBS). The CFBS senses the radio environment and constructs the Radio Environment Map (REM). The REM is used by the CFBS to assign resources to its subscribed users, thus avoiding cross-tier interference. The authors compared two scenarios, 1. in which SUEs sense the radio frequency spectrum and assigns resources to itself based on the sensing results and 2. the proposed CFBS senses the spectrum and allocate resources to SUEs based on the sensing results. The throughput performance of both scenarios was compared to the false alarm probability of the SUE. The results proved that the CFBS based sensing increases the femtocell throughput as compared to the SUEs based sensing due to the fact that SUEs has to sense and allocate the resources thus the overall throughput of the femtocell decreases [13]. The authors however did not consider the mobility of the PUEs which can have a substantial impact on the cross-tier interference. Also, no results on the PUE outage were given in [13].

The idea of obtaining the macro-UE (PUE) scheduling information by the femto-BS from the macro-BS based operating in Orthogonal Frequency Division Multiple Access (OFDMA) is proposed in [25] and [26]. In [25], the authors proposed that a femtocell can avoid interfering with a MUE in the UL and DL if the femtocell uses the Resource Blocks (RBs) of those MUEs that are located far away from it. A femtocell achieves this by first obtaining the MUE scheduling information from the MBS. The scheduling information tells the femtocell which RBs are located to which MUEs. In the next step, the femtocell performs sensing of the spectrum. The result is the knowledge of only those MUEs that are near to it, due to the high signal energy coming from those MUEs. The femtocell then compares both the

sensing and scheduling information and obtains those RBs which are used by MUEs that are far away from it and uses them for its communication. Thus, avoiding cross-tier interference in the DL completely. However, the authors did not consider Rayleigh fading or log-normal shadowing in the communication channel between the femtocell and the MUE which could change the outcome of sensing. In [26] the authors also focused to exploit the user level scheduling information to avoid cross-tier interference from a femtocell to MUEs in the DL only. However, rather than obtaining the scheduling information directly from the MBS, the authors proposed to cognitively sense the user level scheduling information from the MBS by assigning a special identity to the FBS. After sensing the scheduling information the FBS decodes the MUE scheduling information which is encapsulated in the PDCCH (LTE) or DLMAP (WiMax). However, the decoding process is quite complex and also the authors did not consider the impact of fading in their model. In comparison to the approaches above, the authors in [27] proposed a scheme for 3GPP femtocell in which a HeNB does not require an X2 interface connection to the eNB to obtain the MUE resource scheduling information. The scheme is based on DL and UL coupling of the MUE resources. In the proposed scheme, the MUE senses the DL to detect the presence of any HeNBs nearby and if the MUE detects such HeNBs the MUE informs the eNB. The eNB constructs a table in which it puts which of its MUEs is interfered by which of the HeNBs. Once it is done, the eNB schedules its victim MUEs to different DL resources. Based on the coupling of the DL and UL resources the eNB also restricts the UL resources of the MUEs. On the femtocell side, the HeNB senses the UL to detect the presence of any high power MUEs. If the HeNB detects such MUEs, the HeNB stops using those UL resources. The HeNB uses the predetermined

mapping rule to construct the DL scheduling information based on the UL sensing results (DL/UL coupling), and also stops using the DL resources. Hence avoiding interference to the MUEs.

Self organised and self optimised cognitive femtocells have also been proposed in [9]. The basic idea behind the self configuration and optimisation is that a FBS senses the radio frequency spectrum and decides to use the spectrum based on the sensing results, and also due to the fact that the radio environment can change abruptly, the FBS also needs to keep up with the changing radio frequency environment to optimise its network. In [9], the authors propose self organisation and self optimisation schemes to avoid cross-tier interference from OFDMA enabled femtocells to MUEs. A comparison of different sub-channel allocation schemes was performed. In the first scheme, Orthogonal assignment (divide the available spectrum into two parts, one used by macrocell and the other by femtocell). In the second scheme, Co-channel assignment (macrocell and femtocell share the spectrum and interference coordination is neglected). In the third scheme, Co-channel assignment  $FR_x$  (divide the spectrum into  $x$  fragments, macrocell uses all of the spectrum but the femtocell can use only one randomly selected fragment). In the fourth scheme, Co-channel assignment and distributed planning (femtocell use the measurement reports to independently configure its subchannels priority list and the list is updated periodically) and in the last scheme Co-channel assignment and centralised planning (measurement reports are sent by the femtocells to a centralised subchannel broker that plans the frequency usage for femtocells to avoid interference). Out of these sub-channel assignment approaches the authors conclude that the co-channel assignment with centralised planning outperforms the rest in terms of % of successful users, %

of users in outage, macrocell throughput (Mb/s), femtocell throughput (Mb/s) and total throughput (Mb/s). As opposed to the centralised approach adopted by [9], the authors in [28] and [29] proposed a decentralised approach for non co-operative femtocells to self organise and self optimise. In [28] OFDMA based cognitive femtocells was proposed to sense the radio frequency spectrum and assigns spectrum holes based on the sensing results to self organise and avoid interference to macro-UEs. Iterative Water-filling (IWF) power allocation scheme is used to maximise the femtocell throughput. However, no results on the outage probability of the PUE were shown in the paper. In [29], the authors proposed a Cognitive Radio Resource Management (CRRM) scheme to be implemented in OFDMA femtocells. Instead the need for a centralised entity, the femtocell with CRRM can sense the macrocell radio frequency spectrum so as to avoid cross-tier interference. The authors derive the effective capacity of the CRRM that specifies the Quality of Service (QoS) of the system. Based on the effective capacity, the optimum sensing period and radio resource allocation are proposed for the CRRM that ensures high spectrum efficiency along with high QoS of the femtocell. The authors compared the proposed scheme against a randomised scheme in which the femtocell uses RBs in a random fashion and found that the CRRM provides better effective capacity than the randomised scheme. Also, the CRRM ensures low delay bound violation probability for voice streams.

Power control and coverage schemes for cognitive femtocells to avoid cross-tier interference to macro-UEs have also been proposed. A cognitive self optimisation scheme of coverage for femtocell using multi-element antenna is proposed by [30]. The authors proposed to optimise the femtocell coverage area especially at the Critical Places (CPs) in order to avoid interference to macro-UEs and also ensure high

femtocell throughput. For optimisation of femtocell coverage area it is necessary that the pilot power of the femtocell  $P_{femto,pilot}$  is greater than 4dB in CPs so in other location in the architecture, the value of  $\frac{P_{femto,pilot}}{P_{macro,pilot}}$  is above the handover threshold and outside the architecture the value of  $\frac{P_{femto,pilot}}{P_{macro,pilot}}$  is below the handover threshold. The authors achieved this by dividing the femtocell coverage area into 6 sectors and used a 6-element antenna array for shaping the beam and power adjusting to achieve this optimisation. The results are based on the average user's call drop probability and it is seen that the proposed beam shaping approach reduces the call drop probability of the outdoor users and the self optimisation scheme reduces the overall call drop probability of both indoor and outdoor users, hence improved femtocell capacity. However, in this paper the authors only considered path loss in their simulations and no fading or log-normal shadowing was considered which can contribute to sudden fade and a sharp rise in the received signal power measurements at the CPs. Also, no results on the outage probability or interference probability of the macro-UE (PUE) were given. A joint power control and coverage scheme for a cognitive femtocell for throughput maximisation has been proposed by [31]. In this paper the authors proposed to maximise the overall network throughput (macro and femto) by means of power control and coverage assignment. Also, a compensation scheme is introduced in which public users (users served by macrocell) are served by the closed access femtocell. Initially both MBS and FBS measure the received Signal to interference ratio (SIR) from their respective UEs. In the MBS, upon receiving a low SIR than the required threshold, the MBS performs power control in order to improve the SIR from its UE. If the power control does not improve the SIR of the MUE then the MBS assigns the MUE to a FBS. Similarly, at the FBS, initially power control is performed

to improve the SIR from the FUE. If power control does not improve the SIR of FUE, then the FBS looks for another spectrum hole and re-assigns that spectrum hole to its FUE. The authors compared proposed CR femtocell to a conventional femtocell and a conventional macrocell in terms of aggregate throughput (packets/sec), dropped packets due to buffer overflow (packets/sec) and dropped bits due to exceeding retry threshold (bits/sec) and found that the proposed CR femtocell performs better than a conventional femtocell and a conventional macrocell mainly due to the compensation scheme introduced which balances the load between macro-BS and femto-BS.

A scheme to block the RBs that cause interference to macro-users and femto-users is proposed in [32] based on Long Term Evolution Advanced (LTE-A) simulator. In the scheme each macrocell/femtocell identifies the interferer based on the feedback from their users. Also each macrocell/femtocell shares with its neighboring (interfering) macrocell/femtocell, the number of victim users created by it and the total number of users served by it. Based on this co-operation the same RBs used by the macrocell/femtocells are blocked. Thus, no cross-tier interference is caused from femtocells to macrocells and vice versa. The authors in the paper considered only path loss and log-normal shadowing and did not consider fast fading as that can affect the received signal power from either the macrocell or the femtocell.

In [33], the authors proposed to sense the uplink (UL) signal received from the primary user equipment (PUE) and select the best subchannel for the femto-user. The authors used the UL band for both sensing and transmission. In all of the above, only path loss is modeled in the simulations. The effect of fading and shadowing is not included. A Time Division Duplex (TDD) femto scheme operating in UL spectrum was proposed in [18]. UL spectrum was chosen because the position of the PUE's was

unknown and so interference avoidance could not be guaranteed. The primary base station (PBS) position is known and so interference to the PBS can be controlled. Their simulations assumed that femto-PBS interference was negligible, and therefore femtocells must be positioned far from the PBS ( $>1.5\text{km}$ ). This distance constraint is too restrictive as in most cellular systems the link gain is concentrated at the base-station, because of increased antenna gains, higher antenna heights and improved electronics (lower noise figures, and higher transmit powers). This means that the PBS is more susceptible to interference than the PUE. Transmission in the downlink will cause less interference into the primary macrocell. Based on the limitations of the previous work discussed above and especially the work presented by [18], we propose an alternative TDD CR Femtocell Network (CRFN) scheme in the DL macrocell spectrum in Chapter 3. In Chapter 3, the results on CRFN capacity and PUE outage are shown and it is evident from the results that the proposed scheme is very effective in increasing the capacity of the CRFN and also reduces the PUE outage probability.

### **2.4.2 MUE Handover Interference Avoidance Approach**

In situations where non-CR femtocells operate inside a macrocell system, a new solution to avoid cross-tier interference from femtocells to the MUEs in DL must be in place. This is because the interference to the MUE happens when the Received Signal Strength (RSS) from the femtocell is higher than the RSS from the MNB. Thus, this interference can be avoided if the MUE is allowed to handover and move into the coverage area of the femtocell (which was interfering before with the MUE). However, a handover can only take place when the interfering femtocell is operating in either open access or hybrid access mode. This solution to handover the MUE from

the MNB to the “interfering femtocell” avoids the cross-tier interference. However, a potential problem that can arise with this solution is the amount of unnecessary handovers of MUE from MNB to the femtocell [8]. Several authors have proposed handover algorithms and also proposed schemes to reduce the amount of unnecessary handovers of a MUE from MNB to the HNB. In [34], the authors propose handover call flow for 3GPP Universal Mobile Telecommunication System (UMTS) based MNB and HNB. In order to reduce the number of unnecessary handovers between MNB and HNB, a Call Admission Control (CAC) scheme is proposed. Three parameters are considered for CAC: Received signal level, Duration of time in which a MUE maintains the minimum required signal level (threshold time “T”) and Signal-to-interference ( $E_c/I_0$ ) level. If a MUE does not maintain the minimum required signal level within the threshold time “T”, then the HNB does not accept that MUE for a handover. Results with no CAC, T=10s and T=20s are shown and it is evident that for T=20s the number of unnecessary handover is reduced because only those MUEs which maintain the minimum signal level for 20 sec will be considered for handover by HNB. The work presented in [34] also considers interference level for handover decision. Similar work for 3GPP UMTS macrocell and femtocell has been presented by authors in [35]. The authors proposed a slightly different handover call flow as compared to [34]. In addition to the three parameters used for CAC as described in [34], the type of user (pre-registered or un-registered) and capacity (bandwidth) of one femtocell is taken as CAC parameters. Similar simulation parameters as that of [34] were used. In the simulations, the threshold time “T” was given a value of 10 sec and 30 sec. Almost similar results on the number of handover and unnecessary handover probability were obtained. In [36], the authors proposed that the velocity of

the MUE and non-real-time or real-time applications running on MUE are taken as the metric for reducing the number of unnecessary handovers between LTE operated MNB and HNB. If Velocity ( $V$ ) of the MUE is greater than 30 km/h (high speed MUE), then no handover is performed. If  $V > 15$  km/h, and the MUE is running real-time applications then a handover is needed by MUE as the MUE requires high QoS. If a non-real-time application is run by the MUE then there is no need for a MUE handover. However, if  $V > 0$  km/h, the MUE needs a handover. Thus, the proposed handover algorithm based on MUE velocity and service quality (SQ) requirements of the MUE reduces the number of unnecessary handovers and makes the algorithm more efficient than conventional handover. However, the paper did not consider the level of interference on the channels in making handover decisions. Using the same idea of velocity “ $V$ ” of the MUE and the real-time and non-real-time traffic run by the MUE as in [36], the authors in [37] proposed a proactive and reactive handover approach. In a proactive approach, the handover may occur at any time before the level of the Received Signal Strength Indicator (RSSI) of the serving MNB reaches the Hysteresis Margin (HM). However, in a reactive approach the MUE handover from MNB to HNB is delayed even if a suitable HNB is found. The handover is initiated just before the MUE loses connectivity with its serving MNB. In [37], if  $V > 10$  Km/h, then no handover is performed. If  $V > 5$  km/h and the traffic is real-time, then a proactive handover is performed. Otherwise if the traffic is in non-real-time then a reactive handover is performed. If  $V < 5$  km/h and the traffic is real-time, then proactive handover is performed, if the traffic is non-real-time, then reactive handover is performed. The authors in [37] compared the proposed proactive and

reactive approach with each other and with the threshold time “T” approach presented in [34] and found that the reactive handover approach performs better than the proactive approach and the threshold time “T” approach in [34]. The same idea of MUE velocity and traffic conditions on MUE was used by authors in [38] to propose a handover scheme for registered or un-registered users in hybrid access HNBs. An un-registered user is only allowed to perform a handover to the hybrid access HNB if the interference from the MUE reaches above the required UL interference threshold. This scheme reduces the unnecessary handovers.

An Adaptive Hysteresis margin (AHM) to reduce the number of unnecessary handovers between MNB and HNB is presented by authors in [39]. The HM is a well known approach to eliminate redundant handovers, however in this paper the HM is made adaptive based on the Carrier to Interference and Noise Ratio (CINR) received by the MUE from both the MNB and the HNB. The proposed adaptive HM scheme reduces the unnecessary handovers and also increases the DL throughput of the MUEs. The same authors in [40] also proposed adaptive Windowing and Handover Delay Timer (HDT) schemes to reduce the number of unnecessary handovers and also increases the DL throughput. Once again as in [39], the CINR is taken as the parameter to make the Windowing and the HDT adaptive.

Based on the work presented by authors on handover schemes and elimination of redundant handovers, we present a novel handover scheme to avoid cross-tier interference from open access HNBs to MUEs in the DL in Chapter 4. We propose that the HNB causing interference to the MUE will allow the MUE to handover from MNB coverage area into its coverage area. Thus, allowing the MUE to access its network. The HNB only allocates those resources to the MUE which have very low or no level

of DL interference from the MNB. This is achieved by cognitively sensing the DL resources and picking up those resources that have very low or no level of interference. Also, in order to eliminate the redundant handovers between MUE and HNB, a timer “T” is implemented in the MUE. The timer helps to correctly identify the need for a handover. This way the unnecessary requests for handover by the MUE is reduced.

## 2.5 Co-tier Interference Avoidance Schemes

Up until now the focus of the literature review has been to point out the relevant work that has been presented to avoid cross-tier interference from HNBs to MUEs. However, the issue of DL interference from a HNB towards a HUE of a neighboring HNB is also very serious and needs to be dealt with. In this section, relevant work to avoid co-tier interference is presented. This includes CR based approach, Clustering scheme, Beamforming and Frequency reuse. CR has been implemented in HNBs to avoid co-tier interference. In [41], the authors proposed CR enabled interference management for 3G femtocells. The authors proposed an opportunistic channel scheduler which selects the best channel from the interference signature received by the cognitive femtocell. The results indicate lower SINR outage probability with cognitive channel reuse as the number of femtocells increases. A distance dependent path loss channel model was used and no fading or shadowing effects were taken into consideration in the simulations. The same authors in [42] also proposed the CR framework along with an opportunistic scheduler for the UL interference management of 4G femtocells. Once again the effects of fading and shadowing were not taken into consideration in the simulations. In [43], the authors proposed that all HNB use cognitive sniffing to detect whether a neighbor HNB is present or not. Then based on the sniffing result,

the HNB can pick any Component Carrier (CC) as the primary component carrier (PCC). If the PCC cannot satisfy the services required by the UE, then the HNBs choose a Secondary Component Carrier (SCC) based on sharing path loss measurements among neighboring HNBs and selecting the SCC according to the estimated mutual interference.

A graph based clustering approach to manage co-tier interference among HNBs is presented by [44]. A Combination of Frequency bandwidth dynamic division and Clustering Algorithm (CFCA) was proposed. A Femtocell System Controller (FSC) was proposed that obtains all the necessary knowledge of HNB configuration from the macrocell. The entire frequency band is divided into two portions. One portion is dedicated for the MNB use. The other portion is shared between HNB and MNB. The MNB dedicated portion effectively solves the dead zone problem. For the shared portion, a clustering algorithm is proposed which puts the HNBs into clusters based on their geographical locations. Graph theory mathematics is used to put different HNBs into the same cluster. The clustering algorithm allocates femtocells into different frequency reuse clusters and the HNB of the femtocells in the same cluster reuse the same resources while different clusters use different resources. This effectively avoids the co-tier interference between neighboring femtocells. However, the authors only consider path loss and log-normal shadowing in their simulations and no fading is considered. In [45] an energy-efficient interference mitigation scheme is presented for closed access HNBs clustered in a neighborhood area based on their geographical locations. In this scheme, co-tier interference among neighboring HNBs is minimized by reducing the unnecessary Available Intervals (AI) in Low Duty Operation (LDO) mode for HNBs. In the proposed scheme, the neighboring HNBs form a cluster or

are grouped together. In each cluster, one HNB is designated as a leader and other HNBs are designated as members. Only the leader HNB has active AIs in its LDO mode so that any arriving UE can detect the presence of the group by detecting the leader even though the members on the cluster stay in Unavailable Interval (UAI). Once a UE is detected the leader informs the target HNB to activate its AI in the LDO so that the UE can detect the HNB and connect to it. This approach in which only the leader HNB has active AIs in its LDO mode results in minimising the co-tier interference.

Beamforming approach has been studied in [46] to avoid co-tier interference from HNBs to HUEs of neighboring HNBs. In their approach, the authors propose that the victim  $MUE_1$  establishes a control only connection with the aggressor  $HNB_2$  and submits the Channel State Information (CSI) to the aggressor  $HNB_2$ . The aggressor  $HNB_2$  uses transmit beamforming method to steer a null towards the victim  $MUE_1$  using the beamforming weights. This method avoids interference to the victim  $MUE_1$  from the aggressor  $HNB_2$ . However, the trade off is that the  $MUE_2$  served by  $HNB_2$  must have high SINR so that the null steering does not reduce the SINR of  $MUE_2$ . The authors only consider path loss and log-normal shadowing while fast fading affect is completely ignored.

The frequency reuse approach is presented in [47]. In this paper, the authors proposed to divide the whole macrocell frequency band  $B$  into 3 equal parts  $B_{m1}, B_{m2}$  and  $B_{m3}$ . Each of the three sectors of the macrocell use any of the three frequency bands. As an example, sector 1 of the macrocell uses the frequency band  $B_{m1}$ , the femtocells in sector 1 of the macrocell use the frequency band of the sector 2 i.e.  $B_{m2}$  as their centre frequency. The third band  $B_{m3}$  is further divided into three bands  $B_x, B_y$  and

$B_z$ . These frequency bands become the edge frequency band of the femtocells. The radius of the inner circle depends upon how closely the femtocells are located with each other. The authors proposed that the femtocells use the sniffing function to determine which edge frequency band is used by which of its neighboring femtocell and thus allocates its own edge frequency band based on the sniffing results. However, as the behavior of the wireless channel may change anytime due to the effects of fading and shadowing, wrong sniffing results can be obtained by the femtocell and based on those inaccurate results the femtocell may allocate those frequency bands in its outer region which are already allocated by other femtocells in their outside region, thus increasing co-tier interference.

Based on the literature above and particularly [47], in Chapter 5 we propose a resource allocation based co-tier interference avoidance scheme. In our approach we do not divide frequency band into different parts or perform sectoring of the macrocell. In our approach, same frequency is used by the macrocell and the femtocells inside the macrocell. The frequency allocation is performed by a central body called the Femtocell Network Controller (FNC). The proposed resource allocation avoids co-tier interference between femtocells.

## 2.6 Summary

In this chapter, we have highlighted the relevant research undertaken to avoid cross-tier and co-tier interference in femtocell networks. Literature of cross-tier avoidance schemes based on CR is discussed. It was seen that CR enabled femtocells could avoid interference from femtocells to macrocell users by sensing the radio frequency spectrum and avoid using those resources already occupied by the macrocell. Drawbacks

in the literature are also highlighted and it is observed that the papers only considered two of the three channel parameters in simulations. Some paper did not include results for outage probability of the macrocell user. A review of handover schemes to avoid cross-tier interference is also presented. Call flow for MUE handover between MNB and HNB has been discussed in those papers. Also, most importantly, schemes to reduce the amount of unnecessary handovers have also been presented in all of the papers. Schemes to avoid co-tier interference are also presented. These are Cognitive Radio, Clustering of femtocells, Frequency Reuse and Beamforming. In the next chapter, we will present the sensing and transmission scheme that reduces the PUE outage probability and a power control scheme that also increases the femtocell capacity.

## Chapter 3

# Proposed Radio Approach to Avoid Interference from Femtocell to Macro PUE

In this chapter a cognitive radio approach is proposed and utilised in a femtocell in order to avoid cross-tier interference from the femtocell to the Primary User Equipment (PUE) of the macrocell network. The femtocell makes use of the cognitive radio technology to sense and detect any PUEs located near its service area before the femtocell initiates its own transmissions on the DL. The work presented in this chapter has appeared in *PIMRC 2011* [48]. The following are the basis of the proposed radio approach in this chapter

- A sensing and access scheme which enables Time Division Duplex (TDD) operation of an underlay Cognitive Radio Femtocell Network (CRFN) in an Frequency Division Duplex (FDD) macrocell. A Time Division Multiple Access

/ Frequency Division Multiple Access (TDMA/FDMA) system with multiple 200kHz bandwidth channels is considered. The scheme can model the transmission of a Global System for Mobile Communication (GSM)-like system or the RBs of an LTE system, with a similar bandwidth (180kHz).

- The outage performance of the macro cell (the primary system) and the capacity performance of the CRFN (the secondary system) as a function of the Primary Base Station (PBS) to Secondary Base Station (SBS) separation.
- In addition, we consider the effect of multichannel operation of the CRFN for increased throughput. Further improvements are obtained by water-filling the transmit power across the channels.

The remainder of this chapter is organised as follows. Section 3.1 presents the proposed system model, channel model used, proposed sensing and transmission scheme and power control schemes. Section 3.2 provides the simulation parameters and gives results for SBS capacity, SBS channel/slot availability and Primary User Equipment (PUE) outage. Section 3.3 concludes this chapter.

### 3.1 System Model

The proposed system model consists of a macrocell (primary cell) operating in FDD mode, where the DL and UL occupy two separate bands. These bands are divided into channels and furthermore the channels are fragmented into Time Slots (TSs). Each macrocell user is allocated a TS and a channel in a GSM like manner. The model is also applicable to LTE systems where the terminology is Resource Block (RB). The macrocell comprises of a PBS and PUE as shown in Figure 3.1.

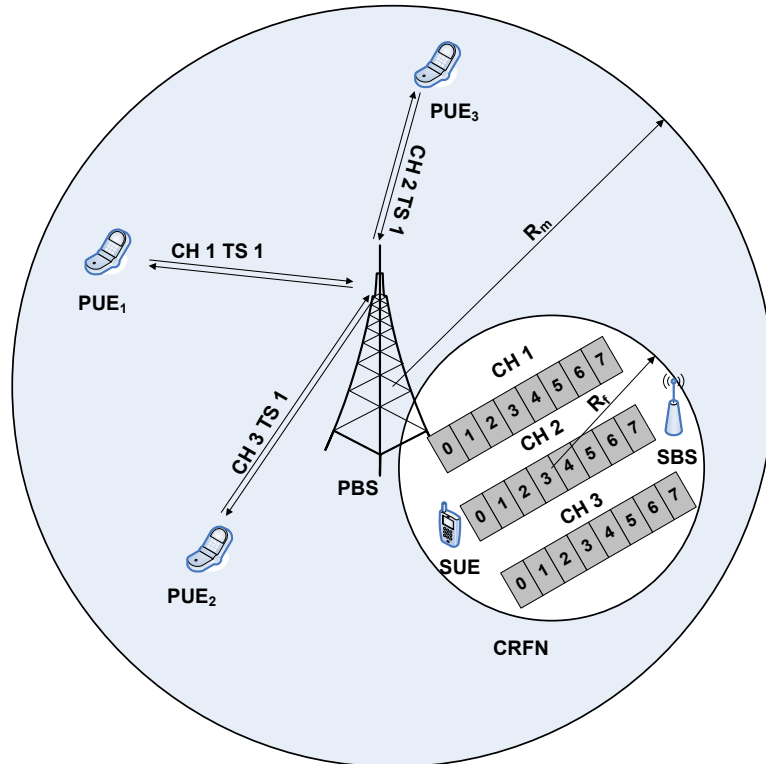


Figure 3.1: System Model consisting of CRFN underlying a GSM network

A CRFN operating in TDD mode is deployed inside the macrocell which comprises of a secondary base station (SBS) and a secondary user equipment (SUE). The PUEs are randomly located inside the macrocell radius  $R_m$ . The CRFN radius  $R_f$  is considerably smaller than the  $R_m$  i.e.  $CRFN_{\pi R_f^2} < PBS_{\pi R_m^2}$ . The transmit power of the Secondary User Equipment (SUE),  $P_{SUE}$  is very low compared to  $P_{PBS}$  and  $P_{PUE}$ , the transmit powers of PBS and PUEs i.e.  $P_{SUE} < P_{PUE} < P_{PBS}$ . The CRFN uses C frequency channels for transmission in the downlink band. This improves throughput and makes up for the loss of uplink spectrum.

### 3.1.1 Sensing and transmission scheme for CRFN

In this section, we propose a sensing and transmission scheme for the CRFN shown in Figure 3.2 and Figure 3.3. The sensing is performed on the UL channel and the

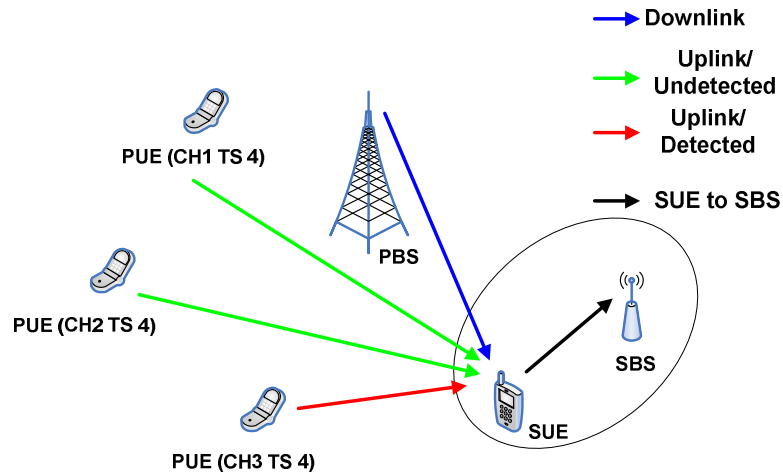


Figure 3.2: Sensing scheme CRFN

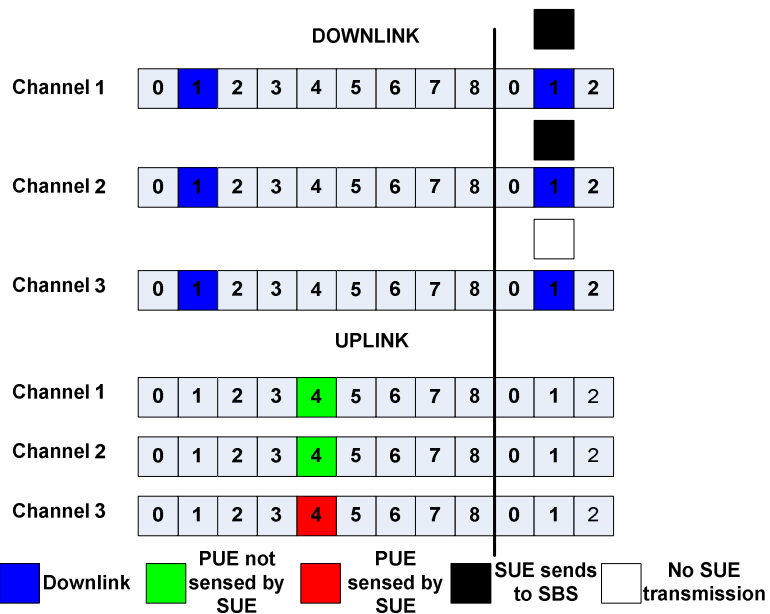


Figure 3.3: Transmission scheme showing  $C=3$  channels,  $N=8$ TSs

transmission is carried out in the corresponding slot of the DL channels. If no signal is detected, then the SUE assumes that the PUE is non-active or it is active but located far from the CRFN. Upon detecting vacant TSs, the SUE will transmit in the corresponding DL TSs. In the case where a PUE signal is detected (as shown in Figure 3.2 for TS 4 of channel 3 the SUE will inhibit transmission in the DL channel, avoiding harm to the nearby PUE. Any transmit power saved is then re-allocated to the remaining TSs (in channel 1 and channel 2).

### 3.1.2 Power Control Schemes

The CRFN employs a multi-carrier scheme using  $C$  frequency channels. It allocates power to these channels simultaneously on the vacant TSs. The total power,  $P_{SUE}$  is distributed either equally among the free channels ( $P_{c,t} = P_{SUE}/C$ ) or water-filled based on the channel gain,  $G_{c,t}$ , and the interference matrix  $I_{c,t}$  received by the secondary receiver. The indexes  $c,t$  represent the available channel and TS respectively.

#### Water-filling Power Control

Water-filling power control [49] and [50] allocates more power to TSs having low interference level and allocates no power to TSs having high interference level [51] as shown in Figure 3.4.

The water-filling approach increases the capacity of the channel. Mathematically,

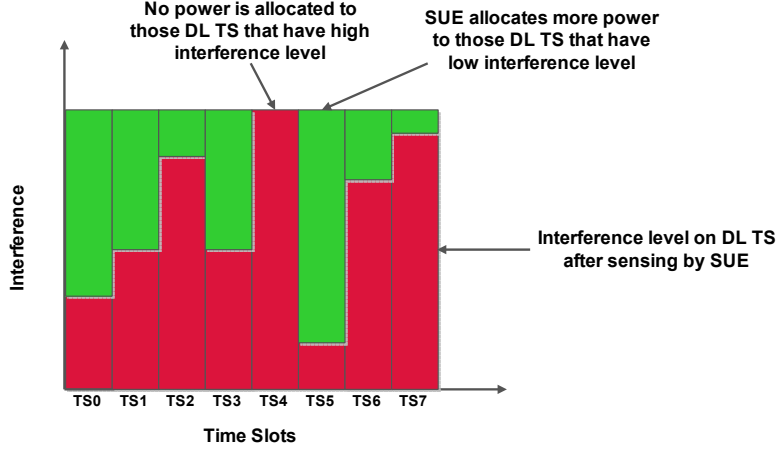


Figure 3.4: SUE water-filling power allocation

the proposed method can be expressed as [52]:

$$\begin{aligned} \max_{P_{c,t}} \sum_{c=1}^C \log_2 \left( 1 + \frac{P_{c,t} G_{c,t}}{(N + I_{c,t})} \right) & \quad (3.1) \\ \text{s.t.} \quad \sum_{c=1}^C P_{c,t} & \leq P_T \\ P_{c,t} & \geq 0, \quad 1 \leq c \leq C \end{aligned}$$

where  $C$  is the total number of frequency channels and  $N$  is the noise. Thus, the power assigned to each channel is according to the expression:

$$P_{c,t} = (\mu - I_{c,t})^+ \quad (3.2)$$

Where  $(x)^+ \triangleq \max(0, x)$ , and  $\mu$  is the water level chosen to satisfy the power constraint with equality  $\sum_c P_{c,t} = P_T$ . The term  $G_{c,t}/(N + I_{c,t})$  corresponds to the channel gain and noise plus interference ratio.  $G_{c,t}$  is the channel gain on a specific TS ( $t$ ) of a channel ( $c$ ),  $N$  is the noise and  $I_{c,t}$  is the interference on a specific TS ( $t$ )

of a channel ( $c$ ). To obtain an estimate of the interference matrix  $I_{c,t}$  an additional sensing step, this time involving the corresponding DL channels (PBS to CRFN receiver), is performed. The SUE feeds back this channel information to the SBS in the control channel as shown in Figure 3.5. As the PBS is in a fixed location and

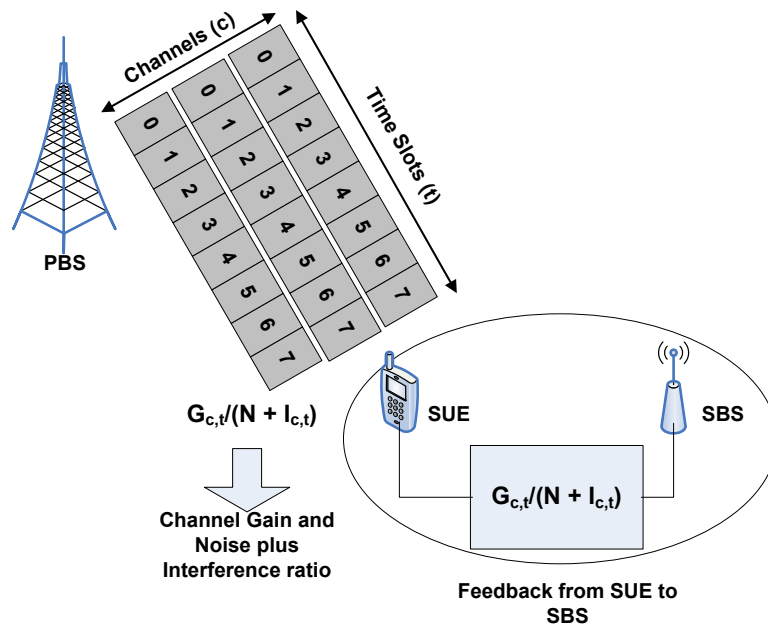


Figure 3.5: SUE feedback to SBS

we assume an almost static secondary network. Therefore, any frequency selective fading can be assumed constant over a number of frames, thus the feedback from the SUE to SBS is not significantly degraded. Note that the “channel reciprocity” which means that the channel conditions between SUE to SBS and SBS to SUE do not vary much, and the TDD nature of the secondary network can be exploited to reduce the feedback requirements from the SUE.

## 3.2 System Parameters and Results

The simulation parameters are shown in Table 3.1. We chose these simulation parameters to model a small size cognitive femtocell network inside a GSM macrocell system. Typical value of cell radius of a small GSM cell ranges from 1 km - 3 km [53]. Thus, a value of 2 km is chosen for the GSM cell radius. The radius of the femtocell cell coverage area is kept at 40m. We assume a system with  $T = 8$  time slots per frame. The PBS transmission power and the PUE transmission power is set to 1W. This much power is needed by the PBS and PUE to successfully communicate with each other especially at the cell edge. The transmission power of the SUE is set to 0.02 W due to the short distance between the SBS and the SUE. Furthermore, as the SUE transmits in DL time slots of the GSM frame, a slight increase in SUE power can result in distorting the signal from the PBS to the PUE in the DL. Typical value of a femtocell transmission power is less than 0.1 W [2]. The SUE sensing threshold  $\gamma_{th}$  is set to 0dB, 10dB or  $\infty$  dB with respect to the noise level. The sensing threshold of 0 dB corresponds to very strict sensing (almost every PUE is detected by the SUE). A 10 dB sensing threshold means that only those PUEs are detected by the SUE that are closer to it (the SUE can then avoid transmission in the DL time slots that are used by the detected PUEs). The sensing threshold of  $\infty$  means no PUE sensing. A receiver with a 5dB noise figure is assumed [27]. Rayleigh fading is used to model the fading channels from PBS and PUE towards SUE. Rician fading with 10 dB K-factor is used to model the fading channel between the SUE and the SBS [54]. In our simulations, outdoor shadowing with 6 dB standard deviation is used to model the signal variations due to the obstacles in the signal path from PBS to PUE and SUE. However, for indoor channel model, the value is reduced to 3 dB as there are

less obstacles in the signal path from SBS to SUE.

Matlab software was used to simulate the proposed sensing and transmission scheme and to calculate the primary outage and secondary capacity as a function of PBS to SBS distance. The simulation was carried out as follows;

- All of the simulation parameters were defined in the Matlab file in the beginning. The number of GSM channels was set to three (any number of GSM channels could be taken, for simplicity we took only 3 GSM frequency channels). Random numbers were generated by using the Matlab's "RandStream" function. The Mersenne Twister [55] "mt19937ar" generator type was specified in the "gentype" in the RandStream function. The program was run for 30,000 iterations.
- The random PUE locations inside the GSM cell were obtained using the "rand" function.
- The sensing of PUE by the SUE is performed and power allocation using waterfilling and equal power is performed.
- Signal to interference and noise ratio at the SUE and PUE are calculated.
- PUE Outage and SUE capacity graphs are obtained from the received signal to noise and interference ratios at the PUE and the SUE respectively.

The simulations were performed using Matlab software. Initially, all the parameters are defined in the Matlab file. Three GSM channels were chosen. A PUE outage occurs if the received SINR  $< 10$ dB. Sensing should stop the outage problem by inhibiting the interfering transmission from the SBS. However, the sensing path PUE

Table 3.1: Simulation Parameters

Simulation Parameters	Notation	Value
Macrocell radius	$R_m$	2 Km
Femtocell radius	$R_f$	40 m
Transmit power PBS,PUE	$P_{PBS}, P_{PUE}$	1 W
Transmit power SUE	$P_{SUE}$	0.02 W
SUE sensing threshold	$\gamma_{th}$	0dB,10dB and $\infty$
Outdoor fading	$F_{out}$	Rayleigh
Indoor fading	$F_{in}$	Rician with K=10 dB
Outdoor Shadowing	$\sigma_{out}$	6 dB
Indoor Shadowing	$\sigma_{in}$	3 dB

to SUE is not reciprocal to the interference path SUE to PUE in terms of Rayleigh fading and so mistakes can be made by the sensing equipment. Note using Figure 3.2 the paths are the same in terms of path loss and shadow fading, but the frequency duplex offset of the UL sensing and the DL transmissions makes the fast Rayleigh fading components uncorrelated. For capacity measurements we use the well known Shannon's capacity formula  $Capacity = (B/T)(\log_2(1 + SNR))$  [56], where B is the channel bandwidth which is 200kHz in our case.

### 3.2.1 Capacity

Figure 3.6 shows the average capacity curves with  $\gamma_{th}=0$  dB,  $\gamma_{th}=10$  dB and  $\gamma_{th} = \infty$  for waterfilling power allocation and equal power allocation. The upper curves show the maximum capacity when there is no sensing at all (the SUE allocates power to all three channels without the knowledge of PUE locations). There is an approximate

20% loss in capacity when sensing is included ( $\gamma_{th}=0$  dB and  $\gamma_{th}=10$  dB). Also shown in Figure 3.6 is the CRFN capacity increase with distance from the PBS. This is intuitive since the macro DL transmissions from the PBS are the major cause of interference. Capacity close to the PBS is particularly poor and drops below 1b/s/Hz when the CRFN is within 350m of the PBS. To some extent, the drop can be mitigated by water-filling which is most effective in this low SINR region, giving an approximate 20% capacity improvement as seen in Figure 3.7. The Figure 3.7 is the zoom of Figure 3.6 and shows that in low SINR region (near the cell center) the water-filling power allocation scheme provides relatively better average capacity than the equal power scheme. The effectiveness of water-filling is reduced as the SINR increases (can be seen from the curves in Figure 3.6 after PBS to SBS distance of 1.5 km). Capacities between 6 and 7 b/s/Hz are available at the cell edge.

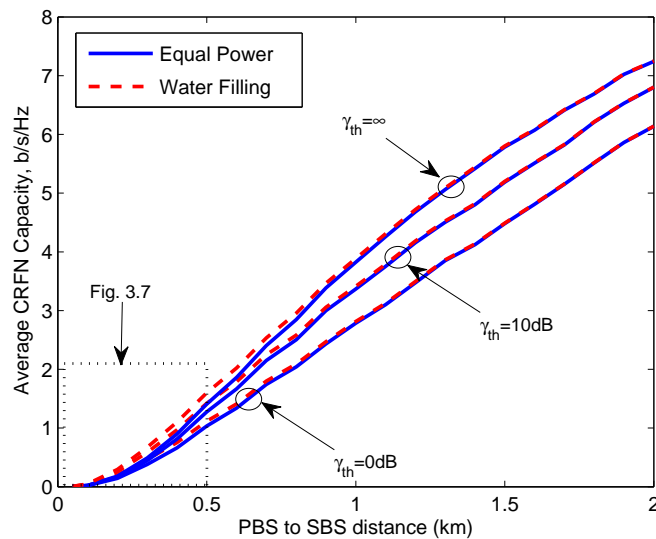


Figure 3.6: CRFN Capacity: Equal power (solid) and Water-filling (dashed) vs SBS to PBS distance with  $\gamma_{th} = \infty$ dB (top), 10dB (middle), 0dB (bottom).

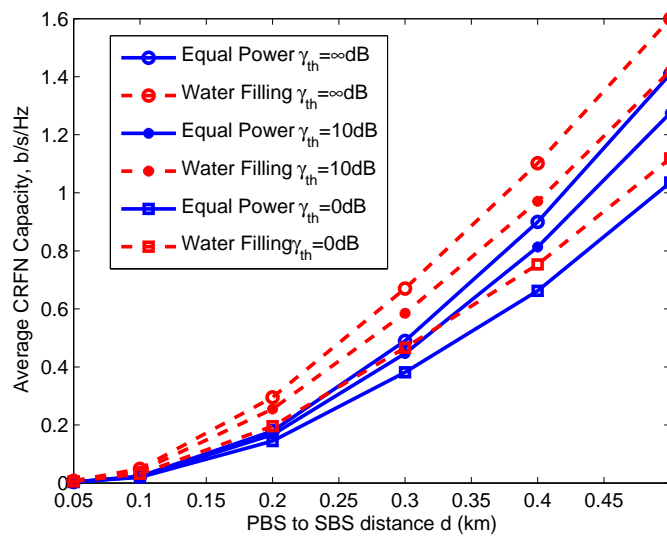


Figure 3.7: CRFN Capacity: Zoom of Fig. 3.6. Equal Power and Water-filling vs SBS to PBS distance.

### 3.2.2 Channel/slot Availability

Figure 3.8 shows how the channel availability is affected by the sensing and water-filling. The equal power curve shows the contribution of the sensing system on channel availability. Sensing stops interference into the primary macro network, but reduces channel availability in the secondary network. At 0dB sensing threshold, channel availability for SUE is about 65% close to the base station and rises to 80% at the cell edge. The increase is caused by the reduced number of PUE's at the cell edge. In practice this effect might not be noticed since there will be other PUE's in adjacent cells with signals above the sensing threshold. When water-filling is added to the system, then some channels (RBs) have too poor a SINR to warrant using any transmission power. These channels become unavailable for transmission and further reduce the channel availability. This is particularly noticeable close to the centre of the macrocell where interference from the PBS is very high and availability drops to

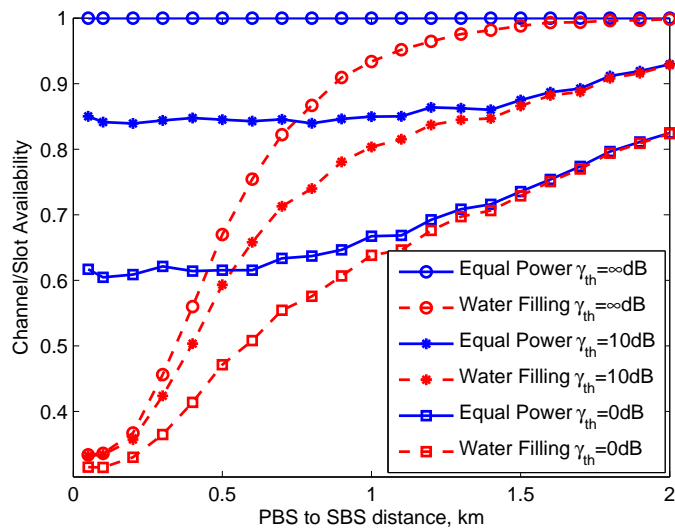


Figure 3.8: CRFN channel/slot availability: Equal Power(full) vs Water-filling (dashed) with  $\gamma_{th} = \infty$ dB(top), 10dB(middle),0dB(bottom).

less than 30%. At the cell edge interference is low, and so channel availability rises until it is just the sensing component contributing to channel unavailability.

### 3.2.3 Primary User Equipment Outage

In case of the Macro PUE outage Figure 3.9, water-filling is shown to have no effect on outage or generate a slightly lower outage probability when the threshold is set high i.e.  $\gamma_{th} = \infty$ dB to minimise the number of inhibited transmissions. From this we understand that from an outage point of view, it is best to concentrate all the transmit power onto a single channel rather than spread the power evenly across all available channels. The  $\gamma_{th} = \infty$  does not inhibit secondary transmissions, so PUE outage increases as the base-station signal gets weaker towards the cell edge. Outage drops at the very cell edge when there is a lower number of PUE's.

The very lowest curve in Figure 3.9 is the natural PUE outage in the cell when

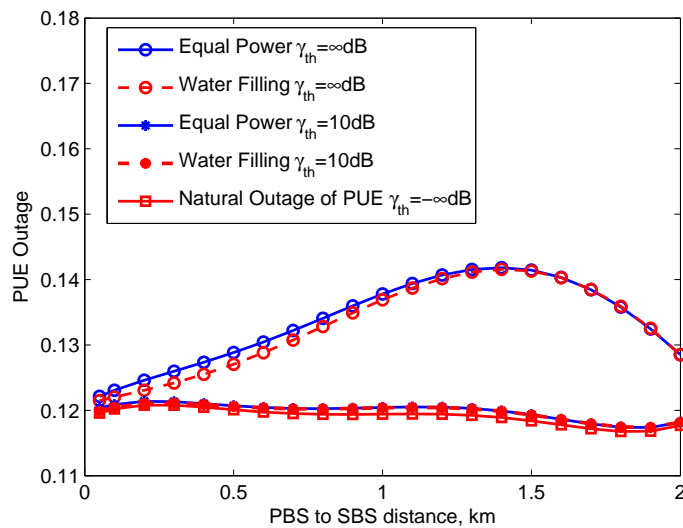


Figure 3.9: PUE Outage: Equal Power(full) vs Water-filling (dashed) with  $\gamma_{th} = \infty$  dB, 10dB,  $-\infty$  dB.

there is no CRFN transmission. As such the outage is caused by noise and fading on the primary path. It is not affected by the position of the CRFN basestation and the average outage over the cell is constant at about 12%. When the CRFN is switched on then there is an additional source of interference. Sensing should minimise this additional interference, and with a sensitive sensing threshold of 0dB, the outage is unaffected except for a minuscule increase at an SBS to PBS spacing of 0.4km (probably caused by the uncorrelated fast fading between the sensing and interference paths as explained above). Even a sensing threshold of 10dB is hardly noticeable being 0.1% above the natural PUE outage. The probability  $P_p(d)$  that a secondary user receives a pilot transmitted by the primary user at a distance  $d$  can be represented as in [57] [58].

$$P_{(p)}(d) = Q_{M_k} \left\{ \frac{P_{PBS} \Pi_k M_k}{N_T d^{2\eta}} \geq \gamma_{th} \right\} \quad (3.3)$$

Where  $P_{PBS}$  is the average transmitted pilot power,  $\gamma_{th}$  is the pilot threshold relative to secondary receiver sensitivity.  $M_k$  are the independant random variables due to propagation effects;  $\eta$  is the propagation constant, when  $\eta=1$ , there is a line of sight between primary and secondary transceiver.  $Q_{M_k}$  is the spatial distribution of the primary users in a given area taking into account the independant random variable due to propagation effects;

$$Q_{M_k} = Q\{SinJ\} = \frac{(\nabla A_J)^s}{S!_J} - e^{\nabla A_J}, S \geq 0 \quad (3.4)$$

$S$  are the SUE in region.  $\nabla$  is the constant representing the spatial density of interfering secondary users.  $A_J$  is the area of a given region  $J$  of SUE deployment.

### 3.3 Summary

In this chapter, we proposed a sensing and transmission scheme for a CRFN inside macrocell. Sensing is done on the uplink channels and CRFN transmission is done on the downlink channels using TDD for two way communications. Parallel transmission on multiple channels increases the throughput. The results are also applicable to LTE-like networks where the RB replaces the channel/TS structure of the GSM network. The proposed sensing and transmission scheme eliminates the sensing-throughput trade off observed in schemes in which sensing and transmission is done on the same TS. For power allocation, we chose two schemes namely equal power and water-filling. The aim was to minimise the outage to the Macrocell and maximise the capacity of the CRFN. From our simulation results we have concluded that water-filling power control scheme only provide improved performance in terms of CRFN

capacity when the CRFN is located close to the Macro BS. The water-filling scheme provides a marginal improvement in PUE outage. Sensing on the other hand is very effective in reducing the additional 2.5% PUE outage caused by the CRFN. Equal power has the advantage of low complexity as no DL interference sensing is required. However, water-filling exhibits high complexity associated with the iterative nature of the algorithm and the additional signaling overhead for the cognitive receivers and DL sensing.

## Chapter 4

### Avoidance of Cross-Tier

### Interference from Open Access

### Femtocells to Macrocell Users

In Chapter 3, a cognitive radio based femtocell was proposed to avoid cross-tier interference from a closed access SBS to a PUE. Sensing was proposed in the SBS before transmission. With sensing the SBS scans the UL frequency spectrum of the GSM system and finds the Time Slots (TS) that are not used by a PUE or are free of any PUE UL transmissions. Based on the sensing results the SBS uses those slots of the DL frame in which no PUE was detected. Thus, cross-tier interference from the SBS to the PUE is avoided. Furthermore, to increase the capacity of the SBS transmissions a power control scheme was also implemented. Waterfilling power control was used by the SBS to allocate power to the TS used in the DL frame according to the SINR value. If a SINR value at the DL TS was high (meaning low interference), more power is allocated to that TS and vice versa. The results showed

that waterfilling power control provides marginal improvement in SBS capacity and the PUE outage. However, the sensing scheme proves to be very useful in lowering the PUE outage even more.

In this chapter, a scheme is proposed to avoid cross-tier interference from TDD open access femtocells to MUE inside a macrocell operating in a FDD mode. A TDMA/FDMA system with multiple 200 kHz bandwidth channels is considered. It can approximately model the transmission of a GSM-like system or the resource blocks of an LTE system, which have a similar bandwidth (180 kHz). Cross-tier interference is avoided by allowing MUEs to handover to the interfering HNB. However, the MUE can only use those TSs or RBs which are vacant and have very low level of interference from the MNB. In order to deal with the problem of increased number of handovers associated with the open access HNBs, a timer is proposed in every MUE. The timer helps to correctly identify the need for a handover. This way the unnecessary requests for handover by the MUE is reduced. In this chapter,

- We describe why a handover is needed by the MUE to the HNB.
- Handover Predication is discussed in which a MNB is able to predict the MUE handover based on the knowledge of the distance between MUE to MNB and MUE to HNB.
- We propose a handover strategy for open access HNBs to avoid cross-tier interference to MUEs.
- Analyse worst case scenario: in which a MUE is interfered by a HNB with no free resources.

- Probability of Macrocell User Equipment (MUE) interference from one Home Node B (HNB) and multiple HNBs is also shown for 100, 500 and 1000 HNBs in the MNB coverage area.
- A novel scheme to reduce the amount of unnecessary handovers of MUE between MNB and HNB is also proposed.

The remainder of this Chapter is organised as follows. Section 4.1 presents the proposed system model and the channel model used. In section 4.2, we propose the solutions to avoid cross-tier interference. Section 4.3 and 4.4 provides the simulation setup and results. Finally, we draw conclusions in section 4.5. The results in 4.4 have been accepted for publication in *JCC 2012* [59].

## 4.1 System Model

The proposed system model consists of a macrocell operating in FDD mode, where DL and UL occupy two separate bands. These bands are divided into channels and furthermore the channels are fragmented into TSs. Each macrocell user is allocated a TS and a channel in a GSM like manner as in Section 3.1. The model is also applicable to LTE systems where the terminology is RB. The macrocell comprises of a MNB and MUE as shown in Figure 4.1.

The MUE moves away from the centre of the cell towards the cell edge randomly with angle  $0 \leq \theta \leq 2\pi$ . The femtocells employ the macrocell DL spectrum in TDD mode. This is done to ensure that no interference is caused to the MNB. The femtocells also operate in open access modes and are randomly deployed in the macrocell coverage area with respect to angle  $0 \leq \theta \leq 2\pi$ . The MNB coverage area consists of  $N$  femtocells.

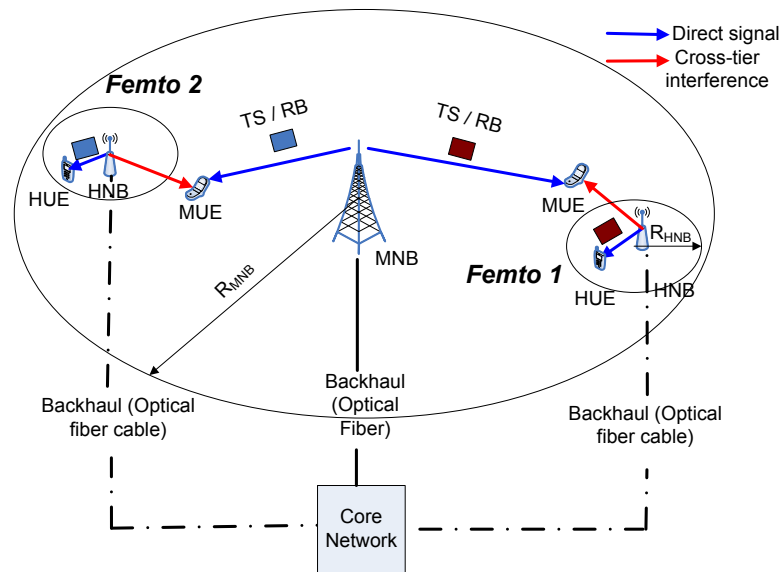


Figure 4.1: System Model: HNBs employing MNB DL spectrum in TDD manner causes cross-tier interference to MUEs

Each femtocell comprises a HNB and a HUE. The HNB coverage radius  $R_{HNB}$  is considerably smaller than the MNB radius  $R_{MNB}$ . The transmit power of HNB,  $P_{HNB}$  is very low compared to  $P_{MNB}$ , the transmit power of MNB. The MNB and HNBs have backhaul connections to the core network (CN) as shown in Figure 4.1. The backhaul is used by the MNB and the HNB to communicate with each other through the CN. The system model also shows the cross-tier interference scenario that results when the HNBs employ the MNB DL spectrum in TDD mode. This chapter focuses on avoiding the cross-tier interference from open access femtocells by allowing MUEs to handover to the aggressor HNB.

## 4.2 Cross Tier Interference Avoidance from Open Access Femtocells

In this section, we describe how to avoid cross-tier interference from TDD femtocells operating in open access mode. As the main advantage of open access mode is the unrestricted access of an MUE to any femtocell having the best Received Signal Strength (RSS). Thus, we propose that if the MUE receives cross-tier interference from femtocells around it, the MUE should handover to the femtocell which has the highest RSS provided the femtocell has interference free RBs to handle the MUE. However, the MUE should be able to correctly identify the need for the handover, as unnecessary handover requests high signalling overheads.

### 4.2.1 Why Handover?

Figure 4.2 shows why we need to handover the MUE to the femtocell. The  $Ec/No$  of MNB at MUE is plotted as the MUE moves away towards the edge of the coverage area (assumed 2 km) in a straight line.  $Ec/No$  is a measure of MNB pilot signal strength to noise and interference.

$Ec/No$  received by the MUE from the MNB can be expressed in terms of pilot and noise powers (in Watts) [54].

$$\frac{Ec}{No} = \frac{p_{pilot}/r_c}{(n_{rx} + i_{sc} + i_{oc})/w} \quad (4.1)$$

Where  $Ec/No$  is the energy per chip (J) divided by the total received noise power spectral density (W/Hz) received by the MUE from MNB.  $p_{pilot}$  is the received pilot power from the MNB in (W). The spread bandwidth is  $w$  (Hz). Thermal noise at

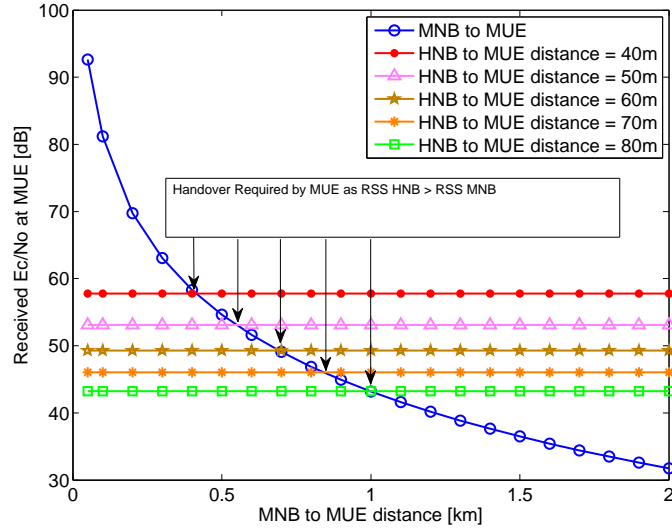


Figure 4.2: Need for MUE handover as it moves away from MNB

the input to the mobile is  $n_{rx}$  (W). The same cell interference is denoted by  $i_{sc}$  and consists of wanted and unwanted signals. The out of cell interference is denoted by  $i_{oc}$ . The  $i_{oc}$  is caused by the HNBs. Since,  $r_c=3.84$  Mcps and  $w=3.84$  MHz, equation 5.1 can be rewritten as.

$$\frac{Ec}{No} = \frac{p_{pilot}}{(n_{rx} + i_{sc} + i_{oc})} \approx \frac{rscp}{rssi} \quad (4.2)$$

Where RSCP is the received signal code power and RSSI is the received signal strength indication. Figure 4.2 also shows  $Ec/No$  values received by the MUE when it is located at different distances from the HNB. The HNBs are uniformly deployed all along the MUE path (0 to 2Km). As the HNB employs the macrocell DL spectrum in TDD mode, the HNB and MNB share the same DL RBs. Initially, we suppose that the MUE moves alongside the HNBs at a distance of 40 m. From Figure 4.2 we see that below the MNB to MUE distance of 300 m, the  $Ec/No$  from the MNB is so

strong that the MUE can stay connected with the MNB even though it is located at the cell edge of the HNB (assumed 40 m). However, as soon as the MUE reaches a distance of 400 m, the  $E_c/N_o$  from the HNB start to become strong. At this point the MUE needs to get connected with the interfering HNB or else the interference might cause it to lose connection with the MNB. Thus, a MNB to HNB handover of the MUE is necessary in order for the MUE to stay connected with the network.

It is interesting to note that if the MUE moved alongside the HNBs at a distance of 50 m, the  $E_c/N_o$  from the HNB becomes strong when the MUE is 540 m away from the MNB. At this MNB to MUE distance a handover is necessary for the MUE to stay connected with the network. Similarly, when the MUE is at 60 m away from the HNB, then the handover needs to be performed at MNB to MUE distance of 700 m. At a HNB to MUE distance of 70 and 80 m, the handover needs to be performed at MNB to MUE distance of 850 m and 1 km. This is because as the MUE to HNB distance increases the  $E_c/N_o$  for the HNB towards the MUE decreases.

Two points are deduced from the above analysis. First, the MUE handover is necessary in order to avoid cross-tier interference from HNB. Second, the MNB to MUE distance at which MUE handover is performed depends upon how far the MUE is away from the HNB. The higher the HNB to MUE distance, the handover has to be performed at higher MUE to MNB distance. For example, see Figure 4.2, when the MUE is located at 20 m away from the HNB, the MUE handover has to be performed at a MNB to MUE distance of  $< 500$ m. However, when the MUE is located at 80 m from the HNB, the MUE handover has to be performed at a MNB to MUE distance of 1 Km. Figure 4.3 provides a pictorial view of MUE handover boundaries with respect to the MNB to MUE distance and MUE to HNB distance.

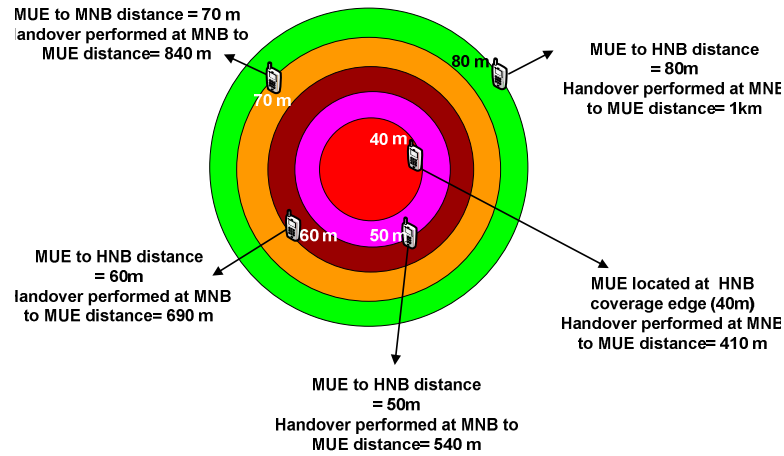


Figure 4.3: MUE Handover Boundries

### Handover Prediction

From the above results one can establish that the MUE handover depends upon MUE's distance from the MNB and also from the HNB. If both the distances are known to the MNB, the MNB can be able to predict the occurrence of a handover without needing the information from the MUE. This is possible in a scenario such as described above where the MUE moves along a straight line towards the edge of the cell, and all along the MUE path HNBs are uniformly deployed. The MNB can obtain exact position of its MUE anywhere in the macrocell in two ways. First, with the help of Global Positioning System (GPS) available in almost every mobile phone. Second, based on the path loss between MUE and itself, and the signal strength measurements sent by the MUE. The HNB locations can be identified by different approaches such as GPS, Cell sensing, TV signals, internet IP addresses and lastly customer address [14]. One can choose any one of those solutions to locate the positions of HNB. Based on this knowledge the MNB is able to calculate the distance of its MUE from the HNB. This way, the signalling load between MUE and MNB is better managed, as the MNB

does not rely on MUE information about RSS measurements to perform a handover.

### 4.2.2 Proposed Handover Strategy for Open Access HNB

In the previous section, we presented that a potential solution to avoid cross-tier interference from an open access HNB to a MUE is to “handover” the victim MUE to the interfering HNB. In [8], the authors propose that if a MUE suffers interference from a HNB in the same channel “C1”, then the macrocell base station performs a channel handover and allocates a new channel “C2” (free of interference) to its user. Unlike in [8], we propose that the MUE be allowed to handover to the open access HNB to avoid the interference from the HNB. The advantages of this scheme are;

- The MUE will receive good quality signal for voice calls and data streaming
- The load on the MNB will be less as after the handover the HNB will provide services to its MUE.

A disadvantage of this scheme is that when the open access HNB is full on capacity (all the resources are already utilised by other mobile users) and the MUE needs to handover to that HNB. A solution for address this challenge is provided in this section. In our proposed scheme a co-channel operation is assumed which means that the HNB uses the same DL RBs as used by the MNB. We also assume that the MNB has a list of all the active open access HNBs in its coverage area which is provided by the CN. The MNB uses this list to identify the HNB likely to cause interference to its MUE. The proposed handover strategy for TDD open access HNB is explained below.

The MUE constantly measures the RSS from the MNB and also from all HNBs in its vicinity. Upon detection of a stronger signal from nearby HNBs than from

its serving MNB on the same shared RB (co-channel), the MUE prepares an RSS measurement report which it sends to the MNB. The MNB makes a handover decision based on the RSS measurement report from the MUE.

$$RSS_{HNB_n} > RSS_{MNB} \quad n = 1, \dots, N \quad (4.3)$$

This report can contain RSS values from multiple HNBs which are likely to cause cross-tier interference to the MUE. In order to avoid this cross-tier interference, the MNB must perform three steps. First step; identify the HNB that is likely to interfere with the MUE. Second step; determine whether the identified HNB in step 1 has a vacant RB to serve the MUE. Third step; handover the MUE to the HNB.

The first step is performed by looking at the RSS measurement report and selecting the HNB having the highest signal strength. For the second step, we propose that all HNBs send their RBs Usage Report (RBUR) to the CN. The RBUR contains the information about which DL RBs are currently utilised and which DL RBs are currently vacant (not being used to serve any user) and have very little or no level of DL interference from the MNB. If a vacant RB has a strong level of interference from the MNB, the HNB does not use that RB for its communication. In order to obtain the information about the level of interference from the MNB on the RBs, we propose that the HNB performs sensing of all the MNB DL RBs. After sensing of all the MNB DL RBs, the HNB can obtain information of interference level on all of its shared RBs with MNB (as HNB employs DL spectrum in TDD mode). The level of interference from the MNB changes due to presence of fast fading in the communication path between the HNB and the MNB.

The MNB requests the RBUR of the HNB selected from the first step. From the RBUR the MNB is able to determine if the selected HNB has an vacant RB. If such a RB is available, the MNB performs step 3 and handovers the MUE to the HNB. If the RBUR indicates no vacant RBs, the MNB selects another HNB from the RSS measurement report satisfying the condition.

$$RSS_{HNB_1} > RSS_{HNB_2} > RSS_{MNB} \quad (4.4)$$

The MNB then requests the RBUR of HNB 2. If an vacant RB is found, the MNB handovers the MUE to HNB 2. In order to avoid unnecessary signalling overheads from HNBs to CN caused by repeatedly sending the RBUR, we propose that the HNBs should update their RBURs only when the state of a RB changes e.g. from “vacant” to “utilised”. This way the CN always has an up-to-date version of RBUR. The proposed handover strategy is shown in Figure 4.4 where the diagram on top shows the proposed steps and information flow. The bottom diagram shows the state of the system after the MNB handovers its MUE to the HNB. An advantage of this handover strategy is the increase in MNB capacity (more users can be accommodated).

The proposed handover process is represented by a flow chart to show the processes, decisions and information flow between MUE and MNB for handover as shown in Figure 4.5. Firstly, the MUE performs RSS measurements both from the MNB and the HNB. If the RSS of MNB is greater than that of the HNB, no handover request is sent from the MUE to MNB. However, if the RSS of the MNB is less than the RSS of the HNB, the MUE starts a timer. After the timer ends, the MUE checks the RSS from both the MNB and the HNB. If the value of RSS from the MNB higher than that from the HNB, no handover requests are sent by the MUE. On the

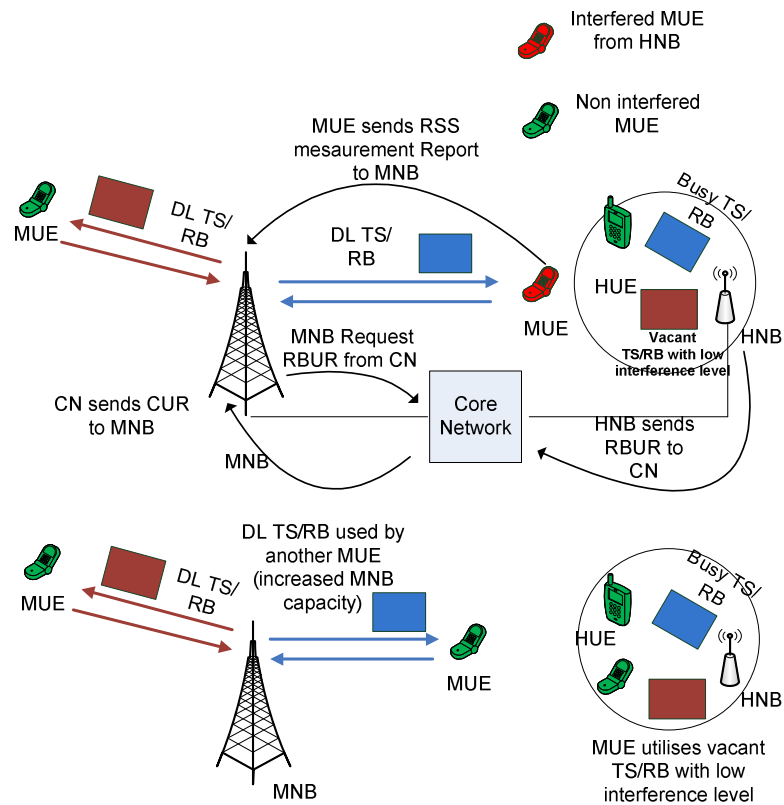


Figure 4.4: Cross-tier interference avoidance for open access femtocells using Handover

other hand, if the value of RSS of the MNB is still lower than that from the HNB, the MUE sends the RSS reports back to the MNB and request a handover to HNB. The MNB requests the CN to provide the RBUR of  $HNB_1$ . If the RBUR of  $HNB_1$  contains RBs that are vacant and have little or no interference levels on them, the MNB initiates the MUE handover. On the other hand, if there are no such RBs in the RBUR of  $HNB_1$ , the MNB looks for another  $HNB_n$  whose RSS is greater than it. If such a HNB is found, the MNB performs handover of its MUE to that HNB (provided the HNB has vacant RBs). If no other HNB is available, the MNB starts a timer and requests RBUR after the timer ends. If the RBUR has vacant RBs, the

MNB performs a handover. Otherwise, the MUE is bound to stay connected with the MNB.

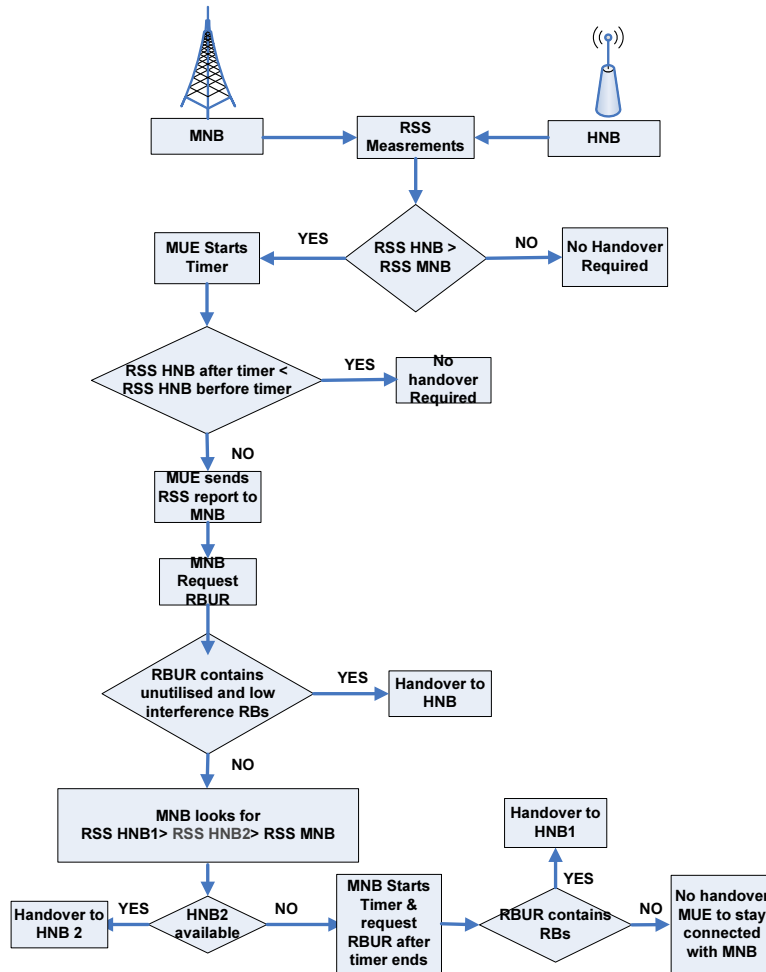


Figure 4.5: Flow chart showing handover processes in MUE and MNB

### Worst Case Scenario: Single Interfering HNB

In the worst case scenario where the MUE is interfered by only a single open access HNB who's RBUR does not contain any vacant RBs, the MUE cannot handover to that HNB. Thus, the MUE has no choice but to stay connected with the MNB. If

however, the MNB can request the RBUR of the HNB again after waiting for a period of time  $T$  (seconds), the MNB might be able to find any vacant RBs. This is because one or more of HNB users might have stopped using the RBs. If a vacant RB is found, the MUE is allowed to handover to the HNB and use that RB. However, if the RBUR still contains no vacant RBs the MUE continues to stay connected with the MNB.

Using Equation 3.3, the probability of interference on a MUE from only a single HNB and multiple HNBs can be derived and shown in Figure 4.6 for 100, 500 and 1000 HNBs. From the Figure, we can see that at low MNB to MUE distance ( $\leq 1.1$

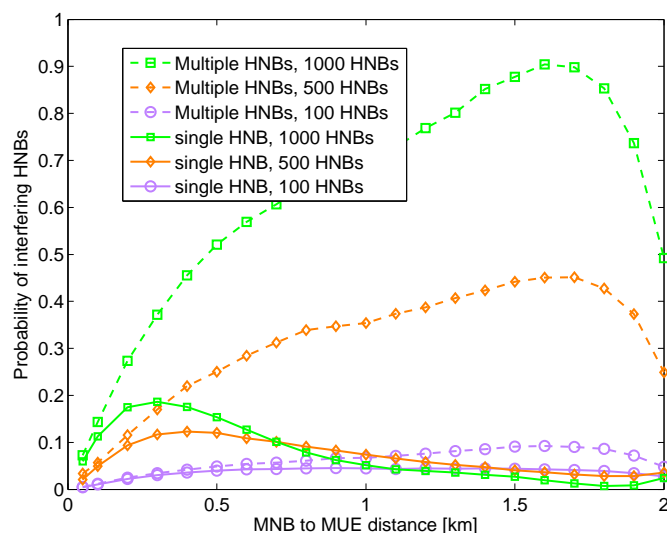


Figure 4.6: Probability of single and multiple interfering HNBs

Km), when the number of HNBs is high, the probability of interference from only a single HNB is also high ( $\approx 20\%$  for 1000 HNBs and  $11\%$  for 500 HNBs as compared to only  $2\%$  for 100 HNBs for a MNB to MUE distance of 300 m). This is because at such low MNB to MUE distance the RSS from the MNB is so strong that most of

the time the MUE is interfered by only a single HNB. However, as the MNB to MUE distance increases from 1.1 km to 2 km, the probability of interference from only a single HNB starts to decrease due to the fact that more and more HNBs starts to cause interference to the MUE. Thus, for a higher number of HNBs this effect is also high which is evident from the Figure 4.6. In the Figure, we can see that beyond 1.1 km, the probability of interference from only a single HNB is very low for 1000 HNBs than 500 HNB and 100 HNBs. In contrast, one can also view the rise in the probability of interference from multiple HNBs as shown in the Figure. From the Figure we can see that the rise in interference probability is highest for 1000 HNBs than for 500 HNBs and 100 HNBs.

The single interfering HNB scenario only holds for a small MNB to MUE distance. Another important observation from Figure 4.6 is that near the cell edge (from 1.8 Km to 2 Km) the probability of multiple interfering HNBs starts to decrease and the probability of single interfering HNBs starts to increase. This is because in that region only a small number of HNBs near the boundary of the macrocell will interference with the MUE as can be seen in Figure 4.8, where the MUE is at the coverage edge of the macrocell, less number of HNBs are in close proximity to the MUE location.

### **4.2.3 Proposed Solution to Minimise Increased Number of Handovers**

As discussed above, the MNB initiates a handover on the request from the MUE. The greater the number of handover requests sent by the MUE, the higher the number of MUE handover routines performed by the MNB. Also, one of the major disadvantages of open access mode is the increase in the number of MUE handovers. If the number

of handover requests put up by the MUE can somehow be reduced, the number of handover routines can also be reduced. In this section we propose a solution that reduces the number of handover requests sent by the MUE to the MNB. A timer  $T$  in milliseconds is proposed in the MUE which helps to reduce the number of handover requests sent by the MUE. The timer has a minimum threshold value  $T_{Min}$  and a maximum threshold value  $T_{Max}$ . The values of  $T_{Min}$  and  $T_{Max}$  are chosen to be very small. In our case  $T_{Min}$  was set to 10 msec and  $T_{Max}$  was set to 30 msec as chosen by [34] and [35] to be 10s and 20s and 10s and 30s. The motivation to use a maximum threshold value of the timer is to see whether the handover requests originated after initial wait of 10 msec can be reduced even further. We chose very small minimum and maximum threshold values to initiate quick “handover or no-handover” decisions from the MUE that leads to quicker handover decision by the MNB. The timer solution works as follows: As soon as the MUE detects a strong RSS from a neighbouring HNB as compared to its serving MNB, the MUE does not send the RSS measurement report to MNB (as in the original scenario), the MUE starts the timer from 0 to  $T_{Min}$ . When the timer ends  $T_{Min}$ , the MUE checks the RSS again. If the RSS from the interfering HNB is below the RSS from the MNB, the MUE does not send the RSS measurement report to the MNB and no handover request is initiated. However, if the RSS of the HNB is still higher than the RSS from the MNB, the MUE starts the timer once again but this time from 0 to  $T_{Max}$ . Once the timer ends, the MUE again checks the RSS. If the RSS is below the MNB RSS level, the MUE does not send any handover request. However, if the RSS is still higher than from the MNB, the MUE sends the handover request to the MNB which then initiates handover procedures which consist of steps 1, 2 and 3. A good

observation from the implementation of the timer is that when the RSS remains high after the minimum and the maximum timer, the MUE can be certain that it is near to a HNB. Thus, a correct handover request is made to the MNB.

The timer is only started when the RSS from the HNB is higher than the RSS from the MNB. This avoids unnecessary use of the timer even when the RSS from the MNB is higher than that from the HNBs. The implementation of the Timer in the MUE results in two advantages. First, the unnecessary transmission of RSS reports to the MNB are reduced, which decreases the signalling load between the MUE and the MNB. Second, the increased numbers of MUE handovers in open access HNBs are reduced.

### 4.3 Simulation Setup

In the simulations, we consider the power relationship between the  $t_x$  and  $r_x$  and account for the propagation characteristics of the channel. The power  $P_{rx}$  received at a distance  $R$  from a transmitter is given by [60] as;

$$P_{rx} = \frac{P_{tx}\Pi_k Z_k}{R^{2b}} \quad (4.5)$$

where  $P_{tx}$  is the average power measured 1 m away from the transmitter. The receiver in our case is the MUE. The Equation 4.5 does not include the noise and interference received at the receiver. Thus, in our case we modify the Equation 4.5 to;

$$P_{MUEr_x} = \frac{\frac{P_{tx}}{N_T}\Pi_k Z_k}{D^{2b}} \quad (4.6)$$

Where  $N_T$  is the total noise ( $N_o$ ) plus interference ( $I_{tot}$ ),  $b$  is the amplitude loss exponent and is site specific and ranges from 0.8-4 (buildings-dense urban environments).  $D_{2b}$  corresponds to the power loss exponent and  $Z_k$  are as used in [60], where  $Z_1=1$  is path loss only,  $Z_1=\alpha^2$  is the path loss and Nakagami fading,  $\alpha^2 \sim G(m, \frac{1}{m})$  denoting a gamma distribution with mean and variance,  $Z_1=e^{2\delta G}$  denotes path loss and log-normal shadowing where  $G \sim N(0,1)$ .  $e^{2\delta G}$  has a log-normal distribution and  $\delta$  is the shadowing coefficient. The  $N(0,1)$  denotes a Gaussian distribution with mean  $\mu$  and variance  $\sigma^2$ . The path loss, Nakagami-m fading and log-normal shadowing has been left out.

The ever changing signal ( $S_F$ ) representation is expressed in time and is written as [60];

$$S_F(t) = \frac{\Pi_k \sqrt{Z_k}}{D^b} \int h(t, \tau) X(t - \tau) d\tau \quad (4.7)$$

$h(t, \tau)$  is the time varying impulse response of the multiple channel and  $X(t)$  is the equivalent transmitted signal. The random variables  $Z_k$  are the slow-varying propagation effects.  $h(t, \tau)$  accounts for the multipath fading.  $h(t, \tau)$  can be expressed as tapped-delay line model given as [60];

$$h(t, \tau) = \sum h_q(t) e^{-j2\pi f_c \tau_q(t)} \delta(\tau - \tau_q(t)) \quad (4.8)$$

where  $f_c$  is the carrier frequency,  $h_q(t)$  and  $\tau_q(t)$  are the time varying amplitudes and delays respectively associated with the  $q^{th}$  multipath.  $\delta(t)$  is the Dirac-delta function.

Table 4.1, presents the simulation parameters used to perform the simulations and are similar to the simulation parameters presented in Table 3.1. In addition, a 15 dBi

Table 4.1: Simulation Parameters

Simulation Parameters	Notation	Value
MNB radius	$R_{MNB}$	2 Km
Number of HNBs	N	100, 500 and 1000
HNB radius	$R_{HNB}$	40 m
MNB Transmit Power	$P_{MNB}$	30 dBm
MNB Antenna Gain	$AG_{MNB}$	15 dBi
Noise Figure	NF	5 dB
HNB Transmit Power	$P_{HNB}$	13 dBm
Outdoor fading	$F_{out}$	Rayleigh
Outdoor Shadowing	$\sigma_{out}$	6-10 dB
Minimum value of Timer	$T_{Min}$	10-15 msec
Maximum value of Timer	$T_{Max}$	20-30 msec

MNB antenna gain was chosen [61]. Furthermore, minimum and maximum threshold value of the timer was chosen as 10 msec and 30 msec [34] [35]. The simulations were performed in Matlab software. Note that in the simulations we considered an MNB or HNB cell to be circular hence the radius parameter despite expressing the  $P_{MNB_{Rx}}$  power in terms of distance.

The simulations were performed as follows;

- All the simulation parameters were defined in the program. The number of femtocells was chosen to be 100, 500 and 1000.
- For the entire MNB to MUE distance, the random positions of HNBs were generated using the Matlab's "rand" function. Furthermore, random positions of a single MUE were also generated.

- Path loss, Rayleigh fading and log-normal shadowing was calculated for the path between MNB and MUE and between HNB to MUE.  $E_c/N_o$  values received by the MUE from the MNB and the HNB are also calculated.
- Sorting of  $E_c/N_o$  from higher to lower values were performed to get a list showing the “highest interfering HNB” and the “lowest interfering HNB”.
- A graph of the  $E_c/N_o$  received by the MUE from the highest interfering HNB was plotted. From the plot the number of handover requests made by the MUE were found out.
- A timer with a minimum and maximum threshold value was defined. Initially, the MUE waits for a threshold time of 10 msec and then performs the RSS measurements (Path loss, Rayleigh fading and log-normal shadowing was again generated to model the ever changing channel characteristics). The new  $E_c/N_o$  values received from the HNBs were recorded and plotted to show where a handover is necessary and where a handover is not required. To further reduce the amount of unnecessary handovers, the MUE waits for a maximum threshold time of 30 msec and then performs the RSS measurements (path loss, Rayleigh fading and log-normal shadowing was again generated). After the maximum threshold time, the MUE again recorded the  $E_c/N_o$  values from the HNB and were plotted to show whether a handover is required or not. Thus, the amount of handovers was reduced by using the timer of minimum and maximum threshold value.

Figure 4.7, 4.8 and 4.9 shows the simulation setup used to model the cross-tier interference experienced by the MUE from femtocells when it moves from the centre

of the cell towards the edge. In Figure 4.7, the MNB is in the middle of the cell. The MUE is near the MNB and 100 HNBs are randomly placed inside the MNB cell. In Figure 4.8, the MUE is shown to have moved away from the MNB and moving towards the cell edge. The MUE movement is random with  $0 \leq \theta \leq 2\pi$ . In Figure, 4.9, the MUE is at the cell edge. Note that in Figure 4.7, 4.8 and 4.9 a femtocell density of 100 have been shown. This is because for 500 and 1000 femtocells all of the MNB cell area would be covered by the HNBs and the MNB and MUE could not have been seen.

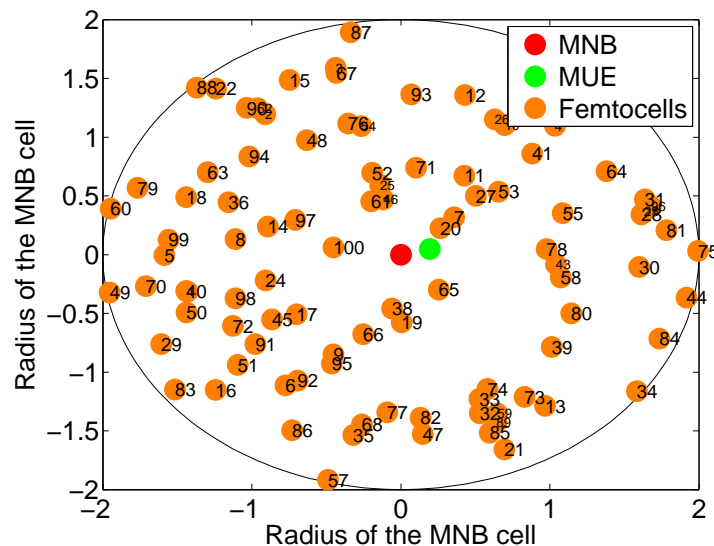


Figure 4.7: Simulation snapshot: MUE at the centre of MNB coverage area

## 4.4 Results

In this section we show how our proposed MUE timer  $T$  helps to reduce the number of increased handovers between MNB to HNB. The results are obtained for 100, 500 and 1000 femtocells. Figure 4.10, 4.11 and 4.12 shows the RSS received by MUE

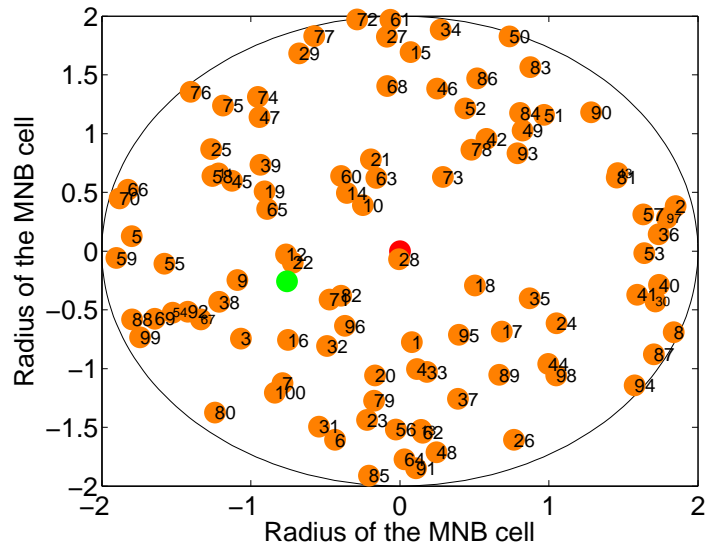


Figure 4.8: Simulation snapshot: MUE at the middle of MNB coverage area

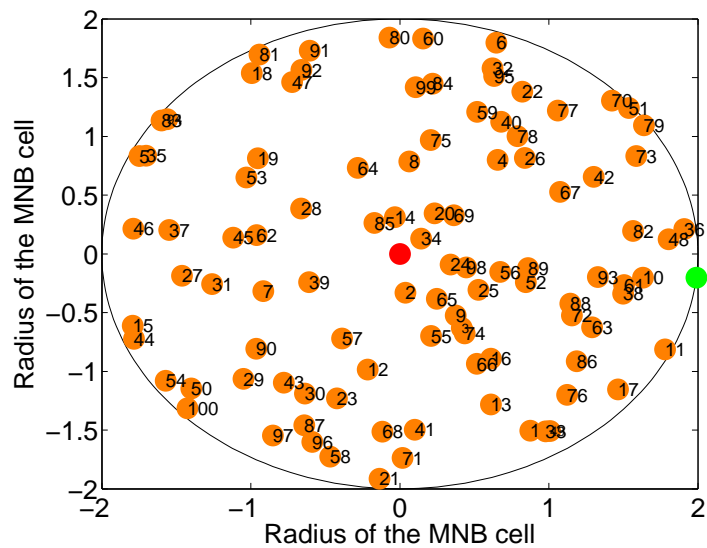


Figure 4.9: Simulation snapshot: MUE at the edge of MNB coverage area

from MNB and the strongest interfering HNB as it moves away from the cell centre towards cell edge. It can be seen from the figures that the  $E_c/N_o$  from the MNB reduces as the MUE moves towards the edge of the cell. However, the  $E_c/N_o$  from

the HNB increases or decreases abruptly due to the channel variations.

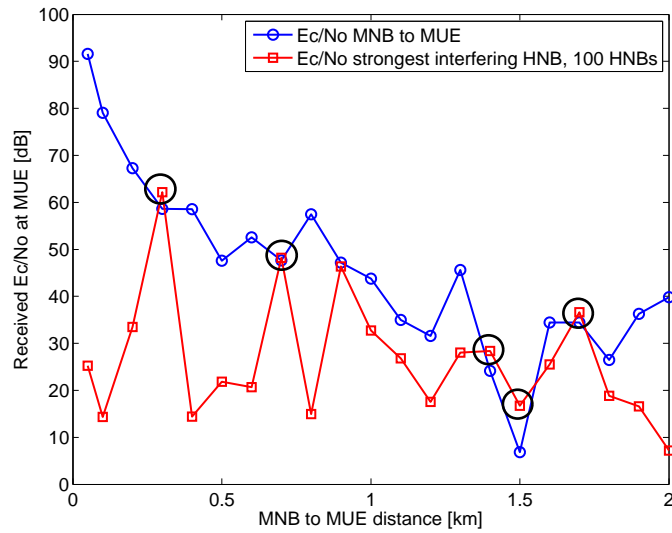


Figure 4.10: 5 handover requests are sent by MUE as depicted by the black circles. Number of HNBs=100

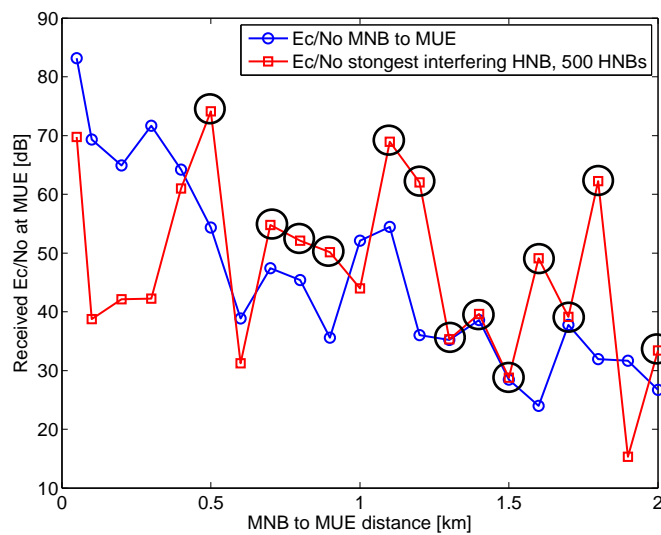


Figure 4.11: 13 handover requests are sent by MUE as depicted by the black circles. Number of HNBs=500

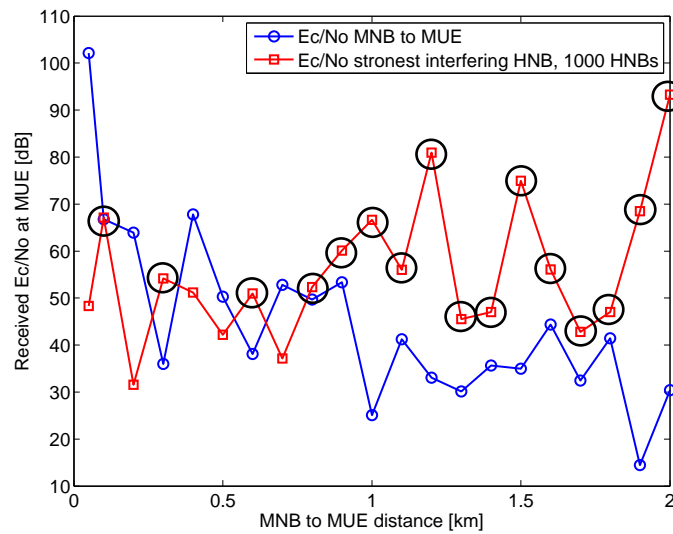


Figure 4.12: 16 handover requests are sent by the MUE as depicted by the black circles. Number of HNBs=1000

As the MUE may receive strong RSS from several HNBs, we only consider the HNBs with the strongest RSS in our case. One can also note from Figure 4.10 that for the case where the MNB coverage area consists of 100 femtocells a total of 5 handover requests are sent by the MUE to the MNB as it moves from the centre of the cell to the edge. With the timer we can see that the number of handover requests are reduced from 5 to just 1 with  $T_{Min} = 10$  msec and with the  $T_{Max} = 30$  msec, the MUE sends no handover request to the MNB as shown in Figure 4.13.

For 500 HNBs, 13 handover requests are sent by the MUE as shown in Figure 4.11. With the 10 msec timer, the number of handover requests are reduced from 13 to 9 (4 handover requests are inhibited) and the 30 msec timer further helps to reduce that number from 13 to 7 (2 extra handover request inhibited) as shown in Figure 4.14.

For 1000 HNBs, the MUE sends 16 handover requests to the MNB as shown in

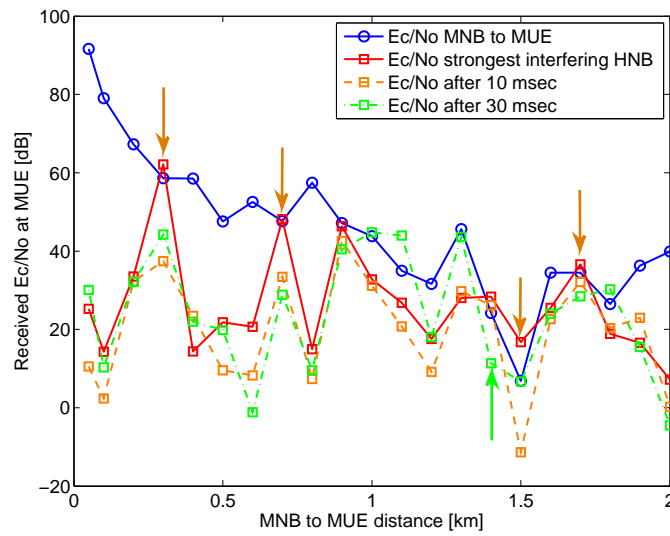


Figure 4.13: Reduced number of handovers after 10 and 30 msec timer for 100 HNBs

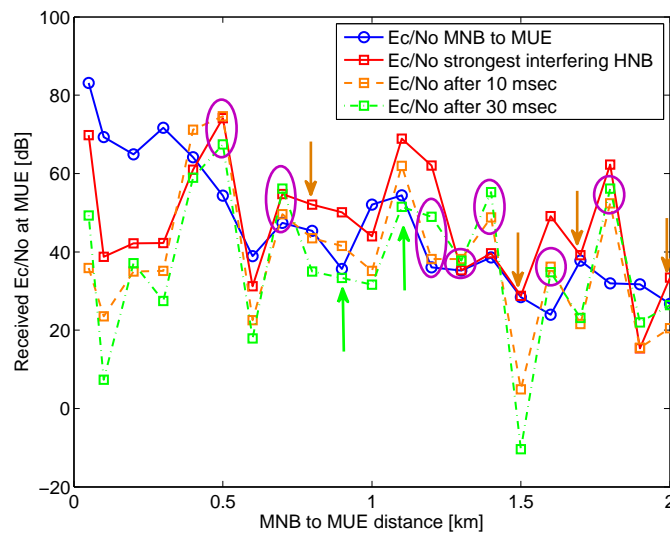


Figure 4.14: Reduced number of handovers after 10 and 30 msec timer. Purple circles show where a handover is necessary. Number of HNBs=500

Figure 4.12. These handover requests are reduced from 16 to just 12 (4 handover requests are inhibited) with a 10 msec delay. A 30 msec delay further reduces the

handover requests from 16 to 11 (MUE inhibits 1 handover request) as shown in Figure 4.15. However, for 1000 HNBs the number of handover request are not reduced significantly. This is because, the higher the HNB density, the greater the chances that the MUE will be require a handover.

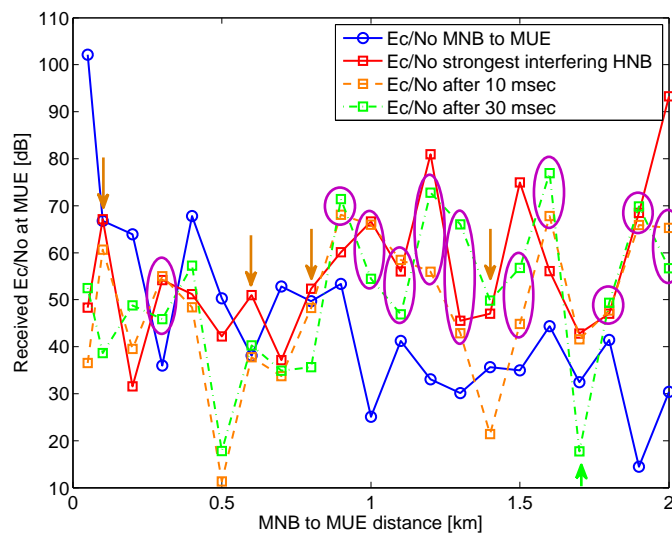


Figure 4.15: Reduced number of handovers after 10 and 30 msec timer. Purple circles show where a handover is necessary. Number of HNBs=1000

The timer makes use of the changes in the channel conditions to correctly identify the need for a handover. The sudden changes in the channel condition which can cause an abrupt increase in the RSS at one instant of time and a sharp decrease in another instant is mainly contributed by the presence of Rayleigh fading between the communication paths. Table 4.2 shows the reduced number of handovers. The presented results will provide guidelines for the operator to understand how the proposed timer can reduce the amount of handovers in small to medium, to a highly dense femtocell deployment

Table 4.2: Reduced number of MUE handover requests

No. of HNBS	No. of Handover Requests sent by MUE		
	Without Timer	$T_{Min} = 10$ msec	$T_{Max} = 30$ msec
100	5	1	0
500	13	9	7
1000	16	12	11

## 4.5 Summary

In this chapter, we have proposed a handover strategy to avoid the cross-tier interference from HNBS to MUE on the shared TDD DL spectrum. The first step is to identify the interfering HNB. The next step is to determine the availability of vacant RBs that have very low levels of interference on them. This RB will be used by the MUE after it handovers to the HNB. For the second step we propose that all HNBS send their RBUR to the CN whenever the state of a RB changes from “utilised” to “vacant”. This helps to reduce signalling load between the HNB and the CN. We also discussed the impact of the number of HNBS on the probability of a single HNB interfering with the MUE, and found out that at low MNB to MUE distance i.e.  $\leq 1.1$  Km, the probability of a single interfering HNB is high for higher number of HNBS. Thus, for 1000 HNBS the probability of a single HNB interfering is 20%, for 500 HNBS it is 11% and for 100 HNBS it is only 2% when MUE is 300 m away from the MNB. It was also observed that as the MNB to MUE distance increased, the probability of single HNB interfering decreased and the probability of multiple interfering HNBS also increased and the increase was directly proportional to the number of HNBS i.e. more than 90% for 1000 HNBS,  $\approx 42\%$  for 500 HNBS and below 10% for 100 HNBS. We also proposed a solution to reduce the number of increased handovers between the MNB and the HNB by implementing a timer  $T$  in the MUE. The timer only starts

when the HNB RSS is higher than the MNB RSS. This approach also reduces the signalling load between MUE and MNB. From the results we can conclude that due to the presence of Rayleigh fading in the communication paths which abruptly shifts the RSS up or down, the proposed timer can make use of this dynamic situation and reduce the number of increased MUE handovers.

## Chapter 5

# Avoidance of Co-tier Interference Between Femtocells With Different Access Modes

In Chapter 4, a handover strategy to avoid cross-tier interference from open access HNBs to MUEs was proposed. A MUE was allowed to handover from the MNB to the interfering HNB provided the HNB possessed interference free channels to serve the MUE once a handover had been performed. Also, a novel scheme to reduce the amount of unnecessary handovers from a MNB to a HNB was also proposed.

Chapters 3 and 4 only considered a cross-tier interference scenarios where a HNB caused interference to a MUE of the MNB. The scenario of co-tier interference (interference between two HNBs) is also an important issue in the deployment of femtocell networks. In this chapter, we propose a novel resource allocation based scheme that avoids co-tier interference from femtocells with different access modes. In particular, we propose a femtocell network controller (FNC) connected to a large density of

femtocells. The FNC acts as a “virtual” macro- base station for the CN and as a “virtual” CN entity for the HNBS. The FNC is responsible for allocating resources to all HNBS that are connected to it. In this chapter,

- We show how co-tier interference originate in planned (ideal) vs. unplanned (realistic) femtocell deployments when only path loss is considered.
- We also show through simulation the effects of co-tier interference between femtocells when fading and log-normal shadowing factors are also included in the communication channel. Fading and log-normal shadowing in addition to path loss gives accurate radius of the Region of Interference (RoI) around a femtocell.
- We propose a resource allocation based on co-tier interference avoidance scheme. Orthogonal resources are allocated to the closed access femtocells while we divide the coverage area of the open access femtocells into two separate coverage areas, inner coverage area and outer coverage area. The inner coverage area is allocated resources that are used by the nearest closed access femtocell while the outer coverage area is allocated resources that are used by the far away closed access femtocells. This resource allocation avoids the co-tier interference completely in the dense femtocell network while the scheme also increases the frequency reuse.

The remainder of this Chapter is organised as follows: Section 5.1 presents the proposed system model and the channel models used; In section 5.2, we describe how co-tier interference is caused in unplanned femtocell deployment; In section 5.3, a

novel resource allocation scheme is presented which aims to avoid co-tier interference between neighboring HNBS; Section 5.4 presents the simulation parameters and setup; Section 5.5 presents the results that compare the interference probability of a HUE with our proposed scheme vs. no resource allocation scheme; Finally, we draw conclusions in section 5.6. The results in 5.5 have been accepted for publication in *IJICTR 2012* [62].

## 5.1 System Model

The proposed system model consists of a large density of femtocells deployed in some area inside the macrocell as shown in Figure 5.1. Specifically,  $N$  femtocells operating

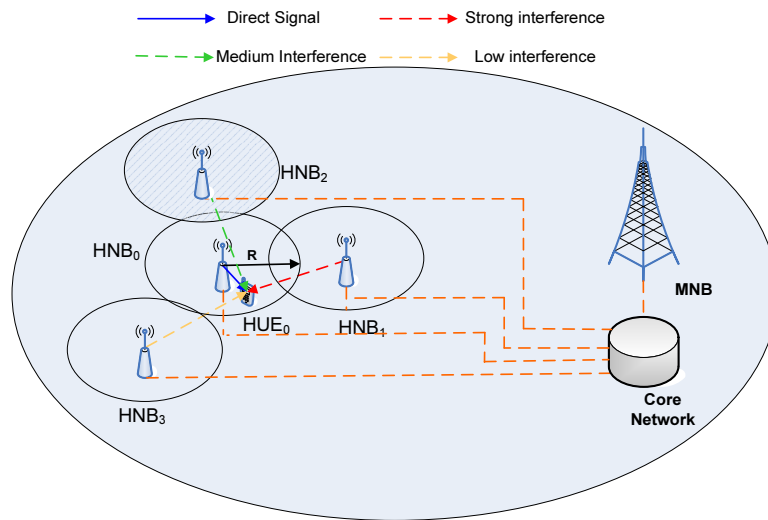


Figure 5.1: System Model

in open and closed access modes are deployed in the macrocell coverage area. The shaded femtocell (HNB) corresponds to a closed access femtocell. The total system bandwidth  $B$  is divided into  $M$  resource block (RB),  $B = MB_{RB}$ . A RB represents a basic time-frequency unit having bandwidth  $B_{RB}$ . Co-channel operation is assumed

where each femtocell uses the same  $M$  RBs. This co-channel operation and the fact that the femtocells are closely located with each other give rise to extreme case of co-tier interference. The system model shows this co-tier interference scenario where HUE of femtocell of interest denoted by  $HUE_0$  being served by the  $HNB_0$  is interfered by HNBS of femtocell 1, 2 and 3. As  $HNB_1$  is located in close proximity to the  $HUE_0$ , the interference from  $HNB_1$  is considered very strong.  $HNB_2$  and  $HNB_3$  are located relatively far away and thus their contribution to interference at  $HUE_0$  is medium to low. The coverage area and transmit power is assumed to be constant for all HNBS. In our model we have only considered the downlink (DL) scenario. The  $E_c/N_o$  received by  $HUE_0$  at RB  $m$  where  $m=1,\dots,M$  is given by [54] as,

$$\frac{E_c}{N_o} HUE_0^m = \frac{p_{pilot} HNB_0^m}{(n_{rx}^m + i_{sc}^m + i_{oc}^m)} \quad (5.1)$$

Where  $p_{pilot} HNB_0^m$  is the received pilot power from the  $HNB_0$  in (W). Thermal noise at the input to the mobile is  $n_{rx}$  (W). The same cell interference is denoted by  $i_{sc}^m$  and consists of wanted and unwanted signals.  $i_{sc}^m$  is  $\approx 0$  in our case. The out of cell interference is denoted by  $i_{oc}^m$  and can be written as.

$$i_{oc}^m = \sum_n^N P_{HNB_n}^m \quad (5.2)$$

Where  $n=1,\dots,N$ . The out of cell interference is the sum of all the signal power at RB  $m$  from  $n$  HNBS. Substituting Equation 5.2 into Equation 5.1 we get,

$$\frac{E_c}{N_o} HUE_0^m = \frac{p_{pilot} HNB_0^m}{(n_{rx}^m + \sum_n^N P_{HNB_n}^m)} \quad (5.3)$$

The Equation 5.3 shows that as the number of interfering HNBs around the  $HUE_o$  increases, the sum of the signal powers from the interfering HNBs on the same resource block “m” increases, which in turns reduces the desired  $HNB_o$  pilot signal on the same resource block “m”. Thus, it is evident from Equation 5.3 that the quality of the  $HNB_o$  pilot is drastically compromised as the out of cell interference increases.

### 5.1.1 Channel Models

The channel models for this chapter are difference from what had been used in chapter 2, because in this chapter interference from one femtocell to another femtocell is studied. As the femtocells have small cell radius, the COST-231 Walfisch Ikegami path loss model that was used in Chapter 3 and Chapter 4 is no longer valid. For small size networks the outdoor and indoor path loss models used are the International Telecommunication Union (ITU) indoor-to-indoor (between HNB to its serving HUE) and indoor-to-outdoor (between HNB to HUE in different femtocell) path loss models [33], where

*Indoor to Indoor channel model*

$$PL_{dB} = 38.6 + 20\log_{10}(d) + 0.7(d) \quad (5.4)$$

*Indoor to outdoor channel model*

$$PL_{dB} = 15.3 + 37.6\log_{10}(d) + WL \quad (5.5)$$

$d$  is in meters, and  $WL$  the is loss due to walls between outdoor HNB and indoor

HUE and is assumed to be 20dB. Rician fading (for indoor to indoor transmissions) is used due to a line of sight between the transmitter and the receiver. Rayleigh fading (for outdoor to indoor transmissions) is adopted alongwith Log-normal shadowing.

## 5.2 Co-tier interference in an ideal (planned) vs reaslistic (unplanned) femtocell network

In this section, we will discuss how the co-tier interference originates between femtocells. Furthermore, we will show how the severity of such interference increases due to close deployment of femtocells to each other. An ideal (planned) femtocell network consists of femtocells whose coverage area does not overlap with the coverage area of other femtocells. An example of such a planned configuration is shown in Figure 5.2. The minimum distance between two HNBs is 80 m. At 80 m, the  $HNB_1$  coverage area is just touching the coverage area of  $HNB_0$ .  $HNB_2$  and  $HNB_3$  are located at 90 m and 100 m away from  $HNB_0$ . The effect of co-tier interference at  $HUE_0$  is observed as it moves away from its serving HNB ( $HNB_0$ ) towards the coverage edge (assumed 40 m).  $E_c/N_0$  is used as a measure of signal strength received by the  $HUE_0$  from  $HNB_0$  and also from  $HNB_1$ ,  $HNB_2$  and  $HNB_3$ . The distance between  $HUE_0$  and the interfering HNB (consider only  $HNB_1$ ) is calculated if we denote the distance between  $HNB_1$  to  $HNB_0$  as  $d_1$  and distance between  $HNB_0$  and  $HUE_0$  as  $d_2$ , thus the distance between  $HNB_1$  and  $HUE_0$  denoted by  $\Delta D$  is written as,

$$\Delta D = \sqrt{d_1^2 + d_2^2 - 2d_1d_2\cos\theta} \quad (5.6)$$

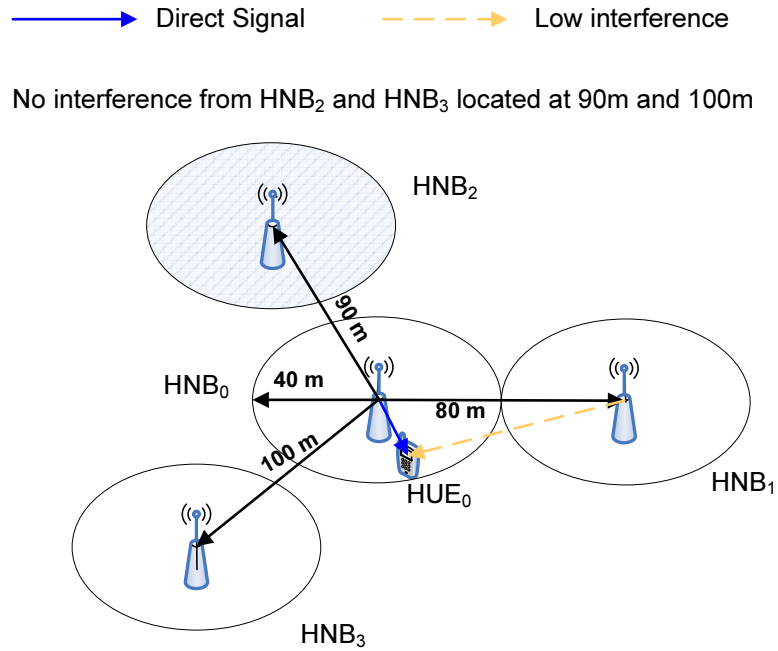


Figure 5.2: Ideal femtocells configuration

Where  $\theta$  is the angle between  $HUE_0$  and  $HNB_1$  and can have value from 0 to 360 degrees. Figure 5.3 shows the distance calculation. From Equation 5.6 the distance between the interfering HNBs and the victim  $HUE_0$  can be found. The co-tier interference from  $HNB_1$ ,  $HNB_2$  and  $HNB_3$  to  $HUE_0$  can be seen from Figure 5.4. From the figure we can see that when the nearby  $HNB_1$  is almost twice the distance of the  $HNB_0$  coverage area, the signal from  $HNB_1$  still leaks into the coverage area of  $HNB_0$  and causes interference to  $HUE_0$  when it is located within 38 to 40 m. However,  $HNB_2$  and  $HNB_3$  have no effect on  $HUE_0$  as they are located quite far from  $HUE_0$ . Thus in an ideal (planned) femtocell network configuration, there are very low chances of occurrence of co-tier interference.

However, in reality, the femtocells are deployed by home users and there is no

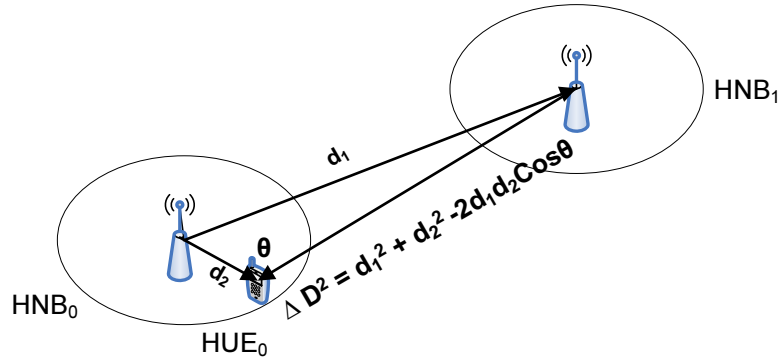


Figure 5.3: Interfering  $HNB_1$  to victim  $HUE_0$  distance calculation

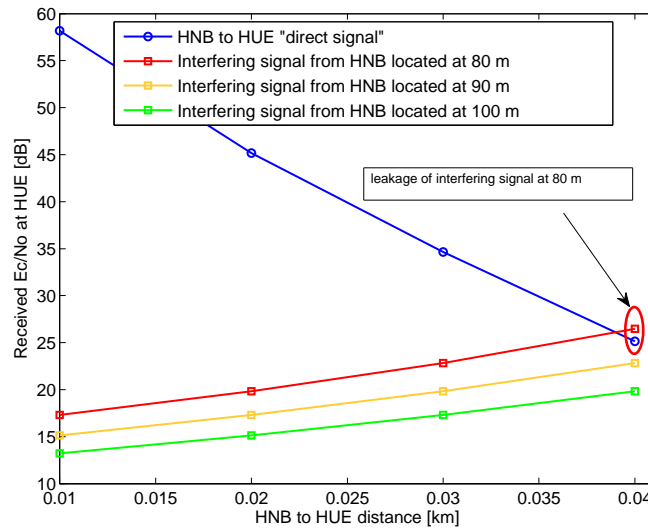


Figure 5.4: Interference due to planned femtocell configuration

network planning performed as done for macrocells, thus the co-tier interference becomes a greater concern. Figure 5.5 shows how the random deployment of femtocells results in co-tier interference. In the figure, HNBs are deployed at random distance around  $HNB_0$ .  $HNB_1$  is located right at the coverage edge of  $HNB_0$ .  $HNB_2$  and  $HNB_3$  are also overlapping the  $HNB_0$  coverage area and are located at 50 m and 60 m away from the  $HNB_0$  respectively.

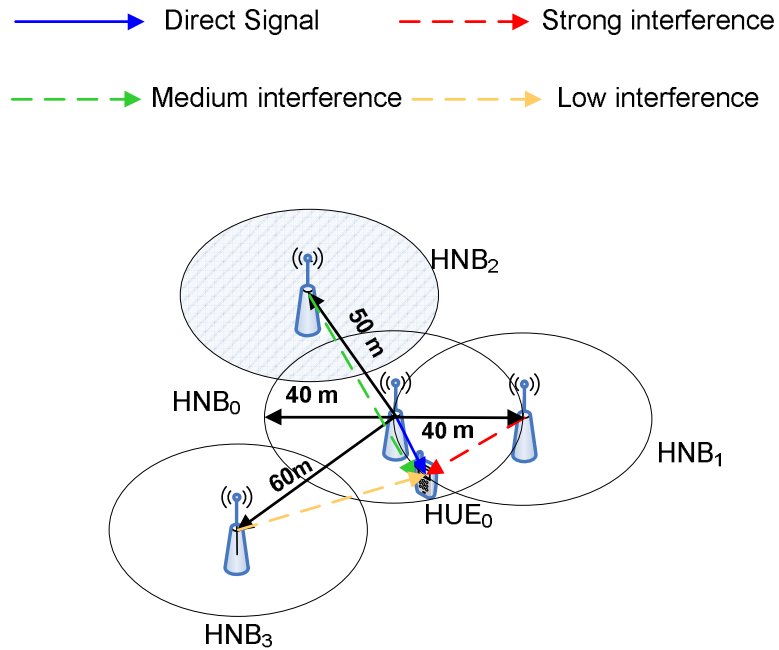


Figure 5.5: Unplanned femtocell configuration

The co-tier interference arising from this unplanned femtocell deployment is shown in Figure 5.6.

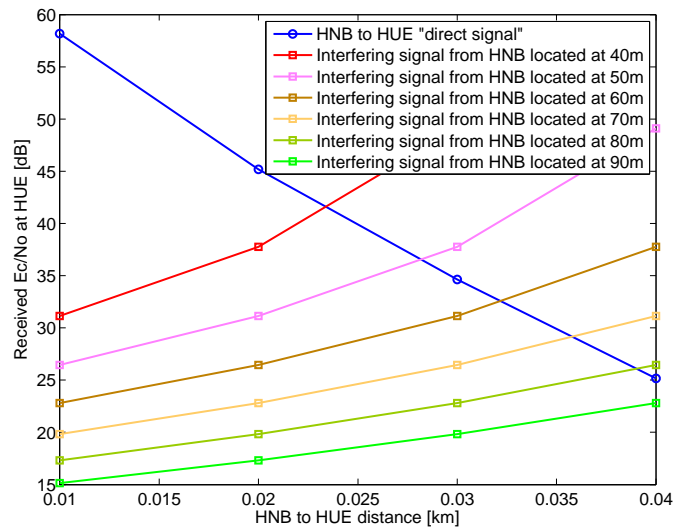


Figure 5.6: Interference due to unplanned femtocell configuration

From the figure, one can see that when the  $HUE_0$  is just under 25 m away from  $HNB_0$ , the  $E_c/N_0$  from  $HNB_1$  becomes strong. This is because  $HNB_1$  is located at the coverage edge of  $HNB_0$ . The  $E_c/N_0$  from  $HNB_2$  and  $HNB_3$  become strong when the  $HUE_0$  is about 30 m and 32 m away from  $HNB_0$  respectively. One interesting observation from Figure 5.4 and Figure 5.6 is that any HNB located at 90 m away from the  $HNB_0$  (having a 40 m coverage area) causes no interference to the  $HUE_0$ . This is due to the high path loss between the interfering HNB and  $HUE_0$ . Conversely, any HNB located within the 90 m region around the  $HNB_0$  will cause interference to the  $HUE_0$ . We call this region the region of interference (RoI). Thus, in our case  $RoI = 90$  m when only path loss is considered. In practical femtocell deployments, the RoI can be calculated by measuring the interference levels from a dummy HNB by varying the distance between the dummy HNB and  $HNB_0$ . The distance from  $HNB_0$  at which the interference from the dummy HNB becomes negligible is the RoI for the  $HNB_0$ . An illustration of the RoI for  $HNB_0$  is shown in Figure 5.7. The out of cell interference received by the  $HUE_0$  at RB m from n HNBS can be written in terms of RoI as in Equation 5.7 where:

$$i_{oc}^m = \sum_n^N P_{HNB_n}^m \text{ for } d_1 < RoI \quad (5.7)$$

and

$$i_{oc}^m \approx 0 \text{ for } d_1 \geq RoI \quad (5.8)$$

Where  $n=1,\dots,N$  is the number of HNBS inside the RoI. From the above Equations, it is clear that if the distance between  $HNB_0$  and the interfering HNBS denoted as  $d_1$  is less than RoI (90m), the  $HUE_0$  will be interfered by them. On the other, hand

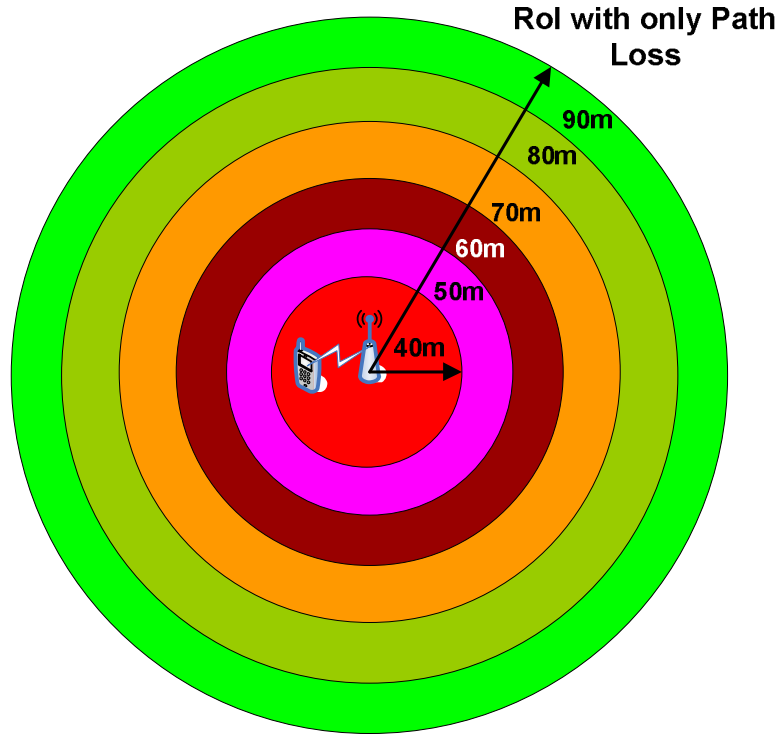


Figure 5.7: RoI with only Path loss

if  $d_1$  is greater than the RoI (90m), no out of cell interference is caused to the  $HUE_0$ .

### 5.2.1 Path Loss, Lognormal Shadowing and Fast Fading

Up until this point, we have analysed the co-tier interference, and also found the RoI for the  $HNB_0$  based on only the path loss between the interfering HNBs and the  $HUE_0$ . With reference to Equation 3.3, we express the probability  $P_{sp}(d)$  that a secondary user detects a primary user at a distance ‘d’, then;

$$P_{sp}(d) = \mathbb{P}_{Z_k} \left\{ \frac{P_{pri} \pi_k Z_k}{d^{2b}} \geq P_{sec} \right\} \quad (5.9)$$

If we use a reference circular region of radius  $(\frac{P_{pri}}{P_{sec}})^{1/2b}$  where  $0.8 \leq b \leq 4$ . Therefore,

$$P_{sp}(d) = \begin{cases} 1, & 0 \leq d \leq (\frac{P_{pri}}{P_{sec}})^{1/2b} \\ 0, & \textit{otherwise} \end{cases} \quad (5.10)$$

Equation 5.10 meets the path loss criteria. However, as we know that there are two other important parameters that can change the channel conditions. These parameters are lognormal shadowing and fast fading. When path loss and log-normal shadowing are taken into account Equation 5.9 reduces to;

$$P_{sp}(d) = \mathbb{P} \left\{ e^{2\sigma G} \geq \frac{P_{sec}d^{2d}}{P_{pri}} \right\} \quad (5.11)$$

Thus, there is also a need to study the effects of co-tier interference on  $HUE_0$  when these two channel parameters are also included in the channel model. In this section, only the unplanned femtocell network configuration of Figure 5.5 is assumed as unplanned deployment is the focus of this chapter. Figure 5.8 shows the  $E_c/N_0$  plots for both the direct signal and the interfering signal received from an interfering HNB located at 40, 50, 60, 90, 110 and at 130 m from  $HNB_0$ . From the figure it is evident that when shadowing and fading are included in the channel model even the HNB located at 90 m away from the  $HNB_0$  will cause interference to the  $HUE_0$ . This was not the case when only path loss was considered (see Figure 6,  $HNB_2$  at 90 m did not cause any interference to  $HUE_0$ ). This shows that shadowing and Rayleigh fading have a great impact on the amount of co-tier interference received by the  $HUE_0$ . From Figure 5.8, the RoI for  $HNB_0$  is found to be 130 m. One can clearly see the effect that the shadowing and fast fading caused in increasing the RoI from 90 m

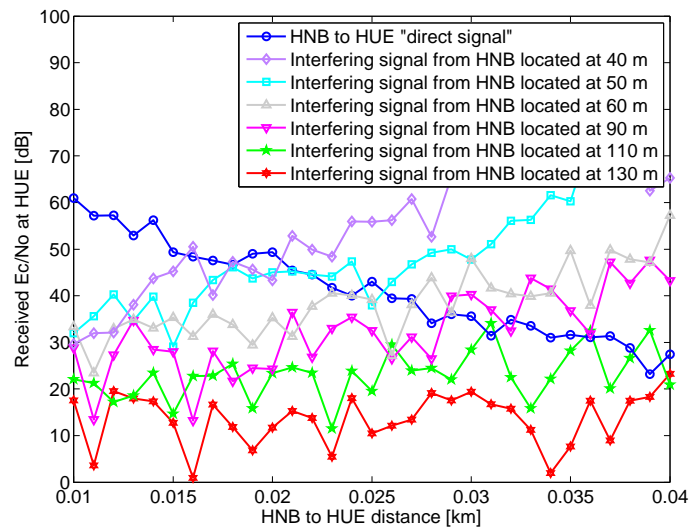


Figure 5.8: Interference due to unplanned femtocell configuration including shadowing and fast fading

(path loss only) to 130 m with path loss, shadowing and fading. An illustration for RoI for  $HNB_0$  is shown in Figure 5.9.

It is to be noted here that the RoI for a  $HNB_0$  can vary depending upon its coverage area as shown in Figure 5.10. It can be seen from the figure that as the  $HNB_0$  coverage area increases, the RoI also increases. This is because as the distance between  $HUE_0$  and the  $HNB_0$  increases, the  $E_c/N_0$  from the  $HNB_0$  reduces further and thus the interfering HNBs located further away will start to interfere with  $HUE_0$ . Rayleigh fading and log-normal shadowing in addition to path loss also play an important role in increasing the RoI for an HNB as shown in the figure.

From the above discussion we can conclude that in a unplanned femtocell network deployment in which the communication channel between the femtocell devices consists of path loss, fading and shadowing, a femtocell located at  $d_1 < 130\text{m}$  will cause interference to the  $HUE_0$  when same RBs are used by both the HNBs. The

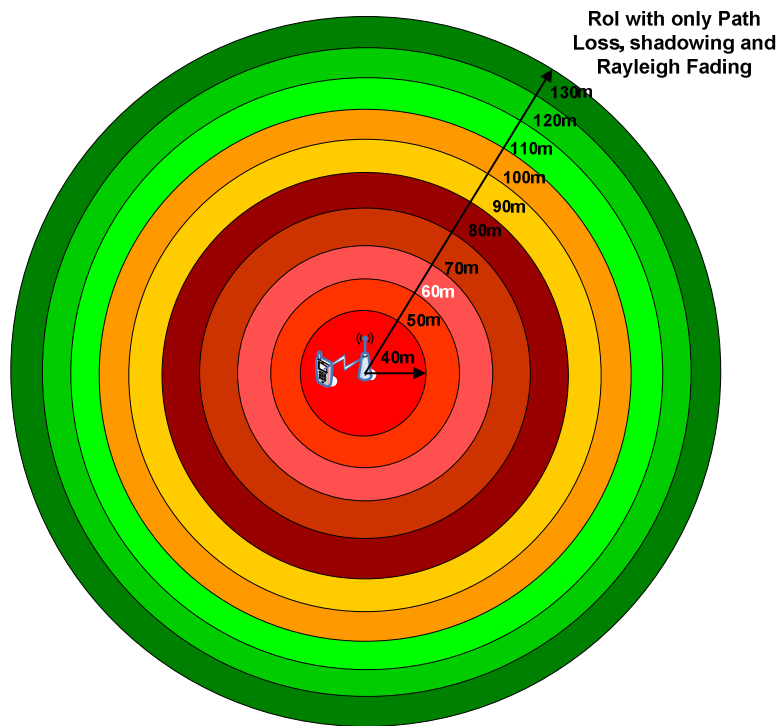


Figure 5.9: ROI with only Path loss, shadowing and Rayleigh fading

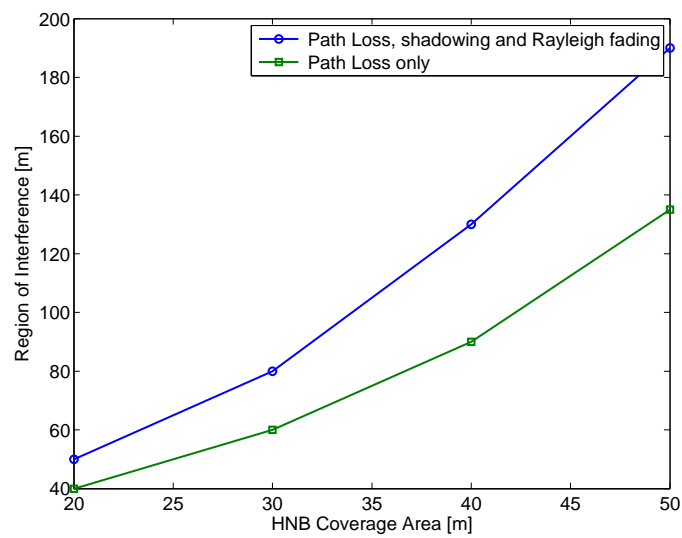


Figure 5.10: Region of Interference versus the HNB coverage area

probability of interference of the  $HUE_0$  is shown in Figure 5.11 when only a single interfering HNB is placed at  $d_1 = 40\text{m}$ ,  $50\text{m}$ ,  $60\text{m}$ ,  $70\text{m}$ ,  $80\text{m}$  and  $90\text{m}$  around the  $HNB_0$ .

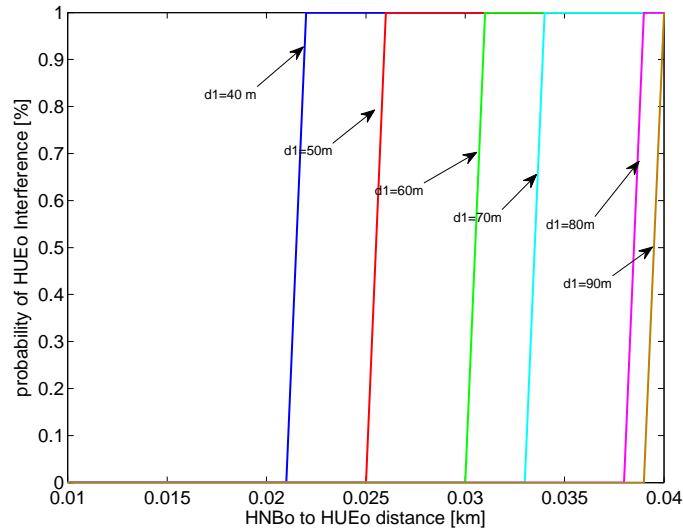


Figure 5.11: Probability of  $HUE_0$  interference from a single interfering HNB

The interference probability is “0” when the  $E_c/N_0$  from  $HNB_0$  towards  $HUE_0$  is higher than the  $E_c/N_0$  from the single interfering HNB and jumps to “1” as soon as the  $E_c/N_0$  from  $HNB_0$  towards  $HUE_0$  is below the  $E_c/N_0$  received from the single interfering HNB. The effect of the interfering HNB at  $d_1 = 100\text{m}$ ,  $110\text{m}$  and  $120\text{m}$  is the same as that of the effect around  $90\text{m}$ . From the figure we can see that when  $d_1 = 40\text{m}$  the  $HUE_0$  gets interfered by the HNB at  $d_2 = 21\text{ m}$ . Similarly, when the interfering HNB is at  $50\text{m}$ ,  $60\text{m}$  and  $70\text{m}$ , the  $HUE_0$  receives interference at  $d_2 = 25$ ,  $30$  and  $33\text{ m}$ . At  $d_1 = 90\text{m}$ , the  $HUE_0$  still receives high interference but we think that the case where  $d_1 = 40$ ,  $50$ ,  $60$ ,  $70$  and  $80\text{m}$  is of most significance. Thus, we change the RoI value from that of  $130\text{m}$  to that of  $80\text{m}$ . The probability of interference from

multiple HNBs located in the RoI of 80 m towards  $HUE_0$  is shown in Figure 5.12. From the figure, it is evident that the  $HUE_0$  experience interference even when the  $HUE_0$  is close to  $HNB_0$  approximately 5% interference. As the  $HUE_0$  moves away from  $HNB_0$  the interference gets severe (approximately 80% at 35 m distance away from  $HNB_0$ ). Thus, it is crucial to avoid this interference for efficient operation of every HNB.

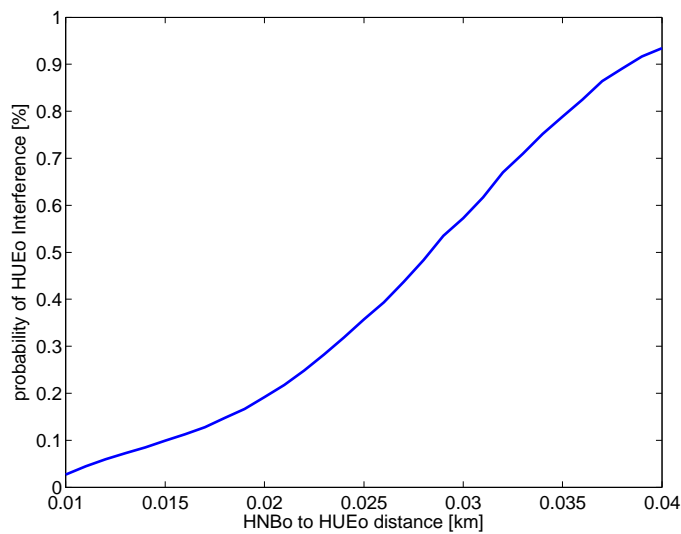


Figure 5.12: Probability of  $HUE_0$  interference from multiple interfering HNBs

### 5.3 Proposed Scheme to Avoid Co-tier Interference

In this section, a solution to avoid co-tier interference is proposed. The solution consists of implementing a FNC in areas inside the macrocell where dense femtocell deployment exists as shown in Figure 5.13.

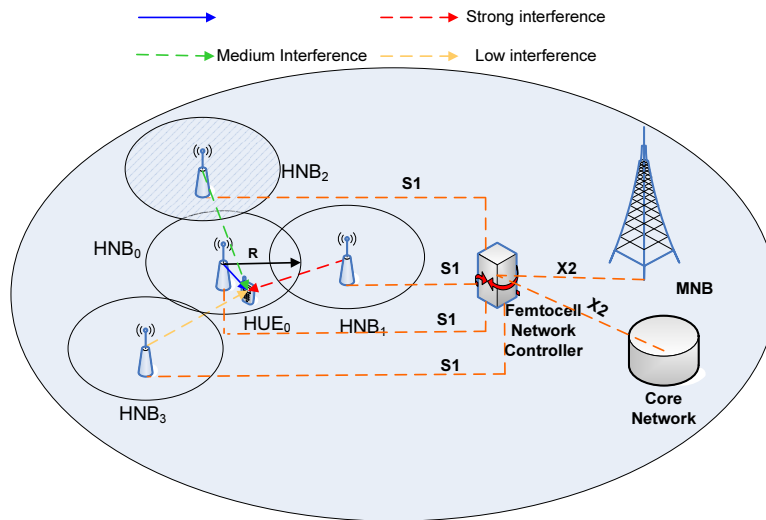


Figure 5.13: Proposed solution incorporating a FNC inside the macrocell

A dense femtocell network can contain 15-20 HNBs located close to each other. The FNC acts as a “virtual” macro-base station for the CN and as a “virtual” CN entity for the HNBs. The FNC can be a part of the network (an HNB can also act as an FNC) or it can be a separate network entity. We assume that the FNC has the knowledge of the positions of all the HNBs and their HUEs connected to it. This is a fair assumption as mentioned in [14], an FNC can obtain knowledge of HNBs positions using GPS. The knowledge of HUE positions is shared by the HNBs with the FNC (using optical fiber backhaul). Similarly, using the same GPS technology, the MNB can provide the location information of its MUEs that are near the dense femtocell network area. Furthermore, the MNB uses the core network to inform the FNC which RBs are used by the MUEs that are near the dense femtocell deployment. This information will be used to allocate resources to the HNBs as discussed in the next paragraph. The FNC has the control over the HNB configuration such as transmit power and resource allocation. The HNBs are connected to the FNC through S1

interface and the FNC is itself connected to the CN and to the MNB via the X2 interface as defined in the LTE standard.

The HNBs connected to the FNC provides it with their Access Modes Identity (AMI). The AMI tells the FNC whether the HNB connected to it is an open access or a closed access HNB. The FNC forms two lists and puts the open access HNBs to one list and the closed access HNBs to the other list. As closed access HNBs do not allow HUEs from other HNBs to connect to it thus it is crucial that the FNC allocates different RBs to the closed access HNBs. This is important as two or more closed access HNBs can be located close together, thus causing interference if same RBs are used among them. This different RB assignment utilises a major portion of RBs. To overcome this and to increase the RB reuse efficiency we propose that the open access HNBs divide their coverage area into two separate coverage area i.e. inner coverage area and outer coverage area. In this scheme the open access HNBs use the RBs allocated to the nearby closed access HNBs in their inner coverage area while they use the RBs allocated to closed access HNBs located far away in their outer coverage area as shown in Figure 5.14. In the figure there are two closed access HNBs ( $HNB_2$  and  $HNB_4$ ) and two open access HNBs ( $HNB_1$  and  $HNB_3$ ) surrounding the femtocell of interest. The closed access HNBs are allocated different RBs as proposed above, while the open access HNBs reuse the RBs allocated to the closed access HNBs. In the figure,  $HNB_0$  is allocated the  $RB_2$  of the closed access  $HNB_4$  in the inner coverage area while it is allocated  $RB_1$  of the closed access  $HNB_1$  in its outer coverage area. Similarly,  $HNB_1$  is allocated  $RB_1$  of closed access  $HNB_1$  in the inner coverage area while it is allocated  $RB_2$  of  $HNB_4$  in its outer coverage area.  $HNB_3$  can be allocated either  $RB_1$  or  $RB_2$  in its inner and outer coverage

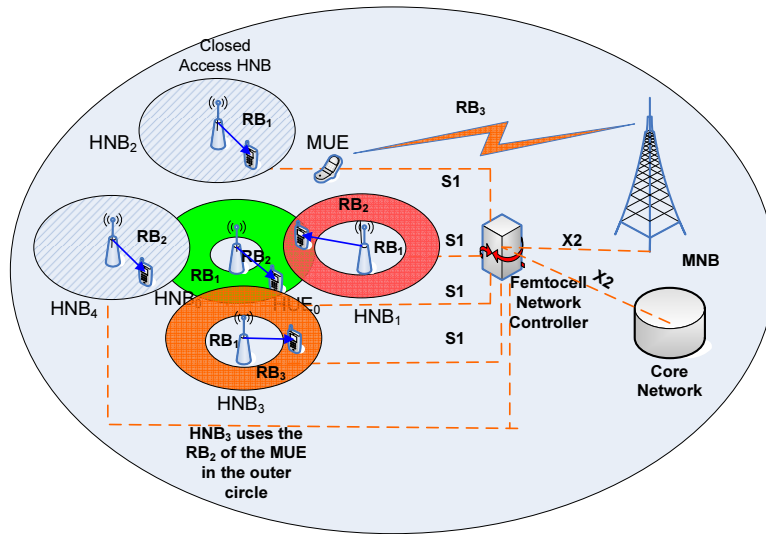


Figure 5.14: Proposed RB allocation scheme

area as both the closed access HNBs are away from it. Another way of improving the RB reuse efficiency is that if an open access HNB can also use the RBs that are allocated to the MUEs near the dense femtocell network area. This can only happen when the MUE is far away from the open access HNB. The open access HNB can use the RB either in the inner coverage area or outer coverage area as shown in Figure 5.14. In the figure,  $HNB_3$  is allocated  $RB_3$  of the MUE as the MUE is far away from  $HNB_3$ . However, in situations where the MUE is near to the open access HNB, the HNB can only use the RB allocated to the MUE in the inner circle in order to avoid it interfering with the MUE. The size of the two coverage areas depends upon the distance between the open access HNB and the closed access HNB and the MUE. The closer the open access HNB is to the closed access HNB or the MUE the smaller will be the size of the inner coverage area and the larger will be the size of the outer coverage area. Note that all of the RB allocation to the closed and open access HNBs are performed by the FNC. The FNC also keeps record of the RBs allocated

to the HNBs in its area so that if a new HNB becomes active it can allocate sufficient resources to that HNB.

In Figure 5.15 we show how the FNC allocates RBs to closed and open access HNBs.

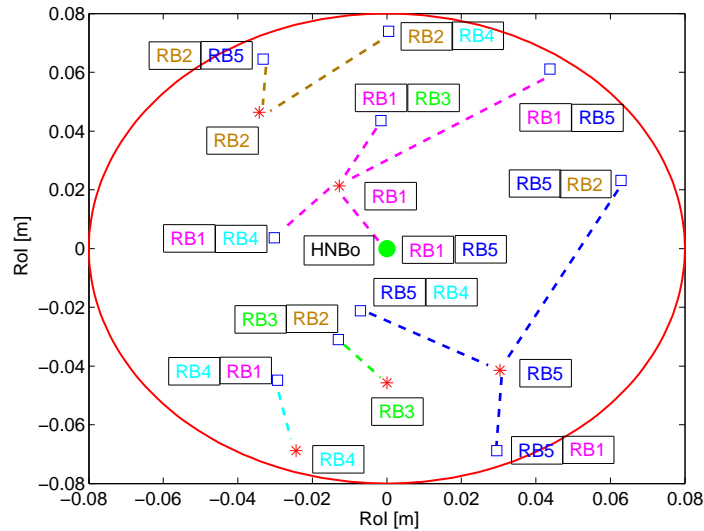


Figure 5.15: RB allocation to open and closed access HNBs

The red stars represent closed access HNBs while the blue squares represent the open access HNBs. The green circle represents the  $HNBo$  of the femtocell of interest. In the figure, the closed access HNBs are allocated orthogonal RBs while the open access HNBs close to the closed access HNBs reuse the RBs of the closed access HNBs in their inner coverage area while using RBs of far away closed access HNBs in their outer coverage area, thus avoiding co-tier interference and increasing the RB reuse efficiency.

Table 5.1: simulation Parameters and Results

Simulation Parameters	Notation	Value
MNB radius	$R_{MNB}$	2 Km
Number of HNBs	N	15-20
HNB radius	$R_{HNB}$	40 m
Noise Figure	NF	5 dB
HNB Transmit Power	$P_{HNB}$	13 dBm
Outdoor Fading	$F_{out}$	Rayleigh
Indoor Fading	$F_{in}$	Rician
Outdoor Shadowing	$\sigma_{out}$	6-10 dB
Indoor shadowing	$\sigma_{in}$	3-6 dB
Region of Interference	RoI	80 m

## 5.4 Simulation Parameters

All of the simulations were obtained by using Matlab software. A table of the major simulation parameters is given in Table 5.1. In our simulations a large density of femtocells were considered inside the macrocell network. Specifically we chose 15-20 femtocells randomly deployed around  $HNB_0$ . The radius of all HNBs including  $HNB_0$  was set to 40m with a transmit power of 13dBm. The  $HUE_0$  was moved from near the  $HNB_0$  to the coverage edge of the  $HNB_0$ . The  $HUE_0$  was moved randomly inside the  $HNB_0$  cell. The HNBs were deployed randomly inside the region of interference (80 m around the  $HNB_0$ ). The positions of the HNBs were also changed to check the efficiency of the proposed FNC based resource allocation. In the Matlab program, path loss, Rayleigh fading, Rician fading and log-normal shadowing was generated. The received  $Ec/No$  at the  $HUE_0$  from  $HNB_0$  and from interfering

$HNB_n$  were calculated. The probability of  $HUE_0$  interference was calculated by dividing the number of times the  $HUE_0$  was interfered by the  $HNB_n$  by the total number of simulations (10,000 simulations in our case). Next, the FNC resource allocation algorithm was run in Matlab which allocates the RBs to the inner and outer coverage area of the open access HNBS as discussed in Section 5.3. The probability of  $HUE_0$  interference was calculated and plotted. Snapshots of the simulation are shown in Figure 5.16 and Figure 5.17. In the Figures the green dots represent the  $HNB_0$  and  $HUE_0$  and the red dots represent the interfering HNBS. Path loss, Rayleigh fading, rician fading and log-normal shadowing were also used in the simulations to achieve accurate results.

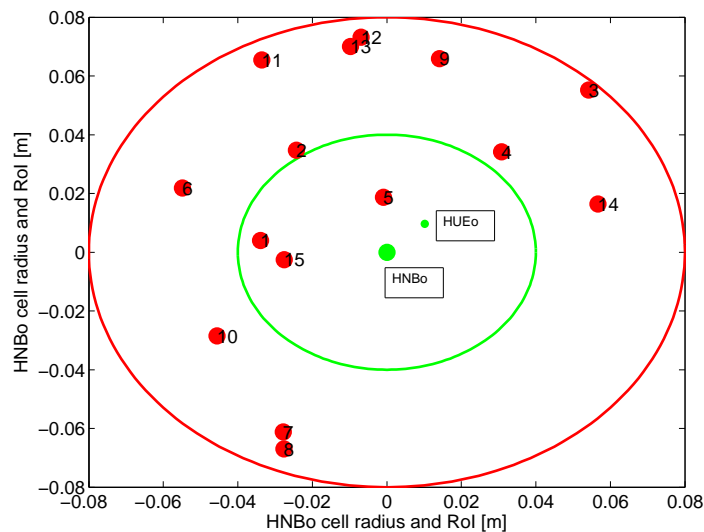


Figure 5.16: Snapshot of  $HUE_0$  near  $HNB_0$

In our simulations we consider that there are 5 closed access HNBS and 10 open access HNBS. The ratio of the closed and open access femtocells can be different. The FNC knows the positions of all the closed access HNBS and allocates orthogonal

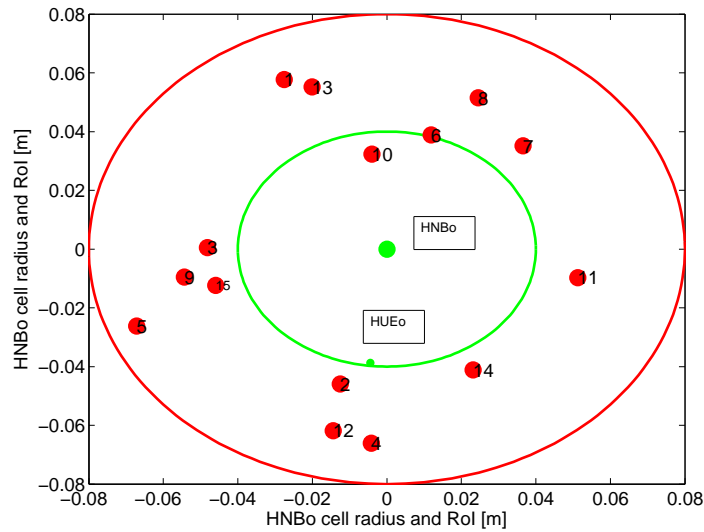


Figure 5.17: Snapshot of  $HUE_0$  at the coverage edge of  $HNB_0$

resources to all of them. The FNC then looks for open access HNBs near those closed access HNBs. The open access HNBs closer to the closed access HNB are allocated the same RBs in their inner coverage area that are allocated to the closed access HNBs, while the RBs of far away closed access HNBs are allocated in the outer coverage area of open access HNBs. Furthermore, the femtocell of interest is also allocated resources according to the procedure above to make sure no interference is caused from the femtocell of interest to other closed or open access femtocells. This novel resource based scheme completely avoids co-tier interference between femtocells having different access modes. The proposed scheme also increases the RB reuse efficiency.

## 5.5 Results

In this section the effectiveness of the proposed scheme is viewed in terms of avoiding co-tier interference and the RBs requirement probability. In Figure 5.18, the interference probability to the  $HUE_0$  with our proposed resource allocation scheme is reduced from 90% at the  $HNB_0$  coverage edge to just 20%. This small amount of interference is due to the Rayleigh fading environment between the  $HNB_0$  and other interfering HNBs using the same RBs in the outer coverage area. The Rayleigh fading sometimes boosts up the signal from the interfering HNB although the distance between the HNBs is large. The result is compared with another frequency allocation scheme [34], and it was seen that their proposed scheme minimises the outage probability from 80% at the cell edge to 20% at the cell edge. However, this 20% cell edge outage probability is only kept for  $HNB_0$  to  $HUE_0$  distance of 10 m. In our case, the proposed scheme can reduce the interference probability to 20% for  $HNB_0$  to  $HUE_0$  distance of 40m. Thus, proving the efficiency of our proposed scheme. In terms of RB requirement probability we can see that in the case where each HNB either closed or open was to be allocated a different RB then for 15 HNBs the FNC needed 15 RBs. The RB requirement was  $\frac{15}{15}=100\%$ . Whereas, with our proposed scheme in which 5 HNBs are closed access and the rest 10 are open access, the RB requirement probability is reduced to  $\frac{5}{15}=33\%$ .

## 5.6 Summary

In this chapter a resource allocation scheme is presented that avoids co-tier interference among femtocells of different access modes. The effects of co-tier interference

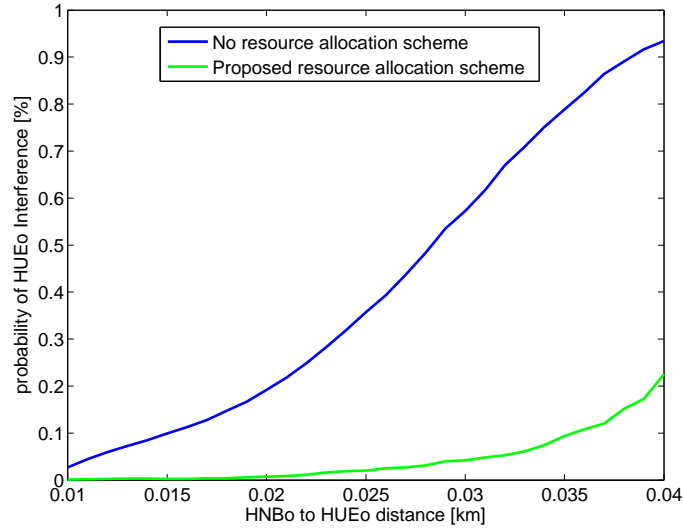


Figure 5.18: Avoidance of interference to  $HUE_o$  from our proposed resource allocation scheme

in an ideal (planned) vs. a realistic (unplanned) femtocell configuration is presented in the chapter. It is observed that the Region of Interference (RoI) estimation based only on path loss was not sufficient to see the effects of co-tier interference. For a 40 m HNB coverage area, with path loss only, the RoI is estimated at 80 m around the HNB. Whereas, when fading and log-normal shadowing is taken into consideration, the RoI increases to 130 m around the HNB. The interference probability of a  $HUE_o$  from a single HNB was simulated. The probability of interference of a  $HUE_o$  from multiple HNBs was also simulated and it was observed that without any efficient resource allocation scheme the interference probability of a  $HUE_o$  reaches to 90% when the  $HUE_o$  is at the edge of its  $HNB_o$  coverage area. In our proposed scheme, a FNC is proposed to manage resource allocation among dense femtocells deployment. The FNC allocates orthogonal resources to closed access HNBs while the coverage area of the open access femtocell is divided into two separate coverage area i.e. inner

and outer coverage areas. The FNC allocates the same RBs in the inner coverage area that are allocated to the closed access HNB nearby while the outer coverage area is allocated those RBs which are used by far away closed access HNBs. This resource allocation among the closed and open access HNBs completely avoids co-tier interference and also increase the RB reuse efficiency.

# Chapter 6

## Conclusions and Future work

In this thesis, we have focused on the avoidance of cross-tier and co-tier interference in femtocell networks. CR technology and handover strategies were used to avoid cross-tier interference from femtocells to macrocell users. Efficient resource allocation scheme was implemented to avoid the effects of co-tier interference in between neighboring femtocells.

In Chapter 1, an introduction to the problem of cross-tier and co-tier interference was presented.

In Chapter 2, relevant literature on the avoidance of cross-tier and co-tier interference was presented. Literature on Cognitive Radio (CR) based cross-tier interference avoidance and literature on Macrocell User Equipment (MUE) handover avoidance schemes was presented. Furthermore, relevant literature on the avoidance of co-tier interference was presented that included CR based approach, Clustering schemes, Beamforming schemes and Frequency reuse schemes.

In Chapter 3, CR technology was implemented in a femtocell to avoid cross-tier interference from closed access femtocells. Specifically, a sensing and transmission

scheme which enables TDD operation of an underlay CR enabled femtocell network in an FDD macrocell was proposed. The sensing scheme avoided the cross-tier interference from femtocell base station to the macrocell user and the access scheme increased the capacity of the femtocell network. The outage performance of the macro cell (the primary system) and the capacity performance of the CRFN (the secondary system) as a function of the PBS to SBS separation was studied. In addition, the effects of multichannel operation of the CRFN for increased throughput was also considered. From our simulation results we concluded that water-filling power control scheme only provide improved performance in terms of CRFN capacity when the CRFN is located close to the Macro BS. The water-filling scheme provides a marginal improvement in PUE outage. Sensing on the other hand is very effective in reducing the additional 2.5% PUE outage caused by the CRFN. The sensing and transmission scheme proposed in Chapter 3 can be extended to the LTE concept. In LTE, the resource block (RB) assignment for a UE is not same on the DL and on the UL channel unlike in GSM. For example, if RB 1 is assigned to a UE in the DL, it is not necessary that the same RB will be assigned to the same UE in the UL. The Physical Downlink Control Channel (PDCCH) provides the UL and DL resource allocation to the UE. The base station sends the PDCCH to every UE. Based on the PDCCH information and our proposed sensing and transmission scheme, the cognitive femtocell can use the same RBs without causing any interference to the other UEs.

Chapter 4, presented an approach for avoiding cross-tier interference from open access femtocells based on MUE handover from MNB to HNB (for GSM and LTE networks). The idea was that whenever the value of RSS at the MUE from the HNB and its serving MNB is  $RSS_{HNB} > RSS_{MNB}$ , the MNB performs a handover of the

MUE to the HNB with the high RSS to avoid interference from that HNB to the MUE. Also, a handover predication mechanism is discussed in which a MNB is able to predict the MUE handover based on the knowledge of the distance between MUE to MNB and MUE to HNB. A worst case was also discussed in which a MUE is interfered by a HNB with no free resources. Probability of MUE interference from one HNB and multiple HNBs was also shown for 100, 500 and 1000 HNBs in the MNB coverage area. A novel scheme to reduce the amount of unnecessary handovers of MUE between MNB and HNB was also proposed. with our proposed “Timer” scheme the number of unnecessary MUE handover requests were reduced from 5 to just 1 for  $T_{Min} = 10$  sec and 0 for  $T_{Max} = 30$  sec for 100 HNBs. For 500 HNBs, without timer, 13 requests were sent from MUE to MNB, only 9 with  $T_{Min} = 10$  sec and only 7 (two more reduced) with  $T_{Max} = 30$  sec. For 1000 HNBs, without timer, 16 requests were sent by MUE to MNB while only 12 were sent with  $T_{Min} = 10$  sec, and 11 with  $T_{Max} = 30$  sec.

In Chapter 5, a novel resource allocation scheme was proposed to avoid co-tier interference between neighbouring femtocells having both closed and open access modes in an LTE network. In that chapter we showed how co-tier interference originate in planned (deal) vs. unplanned (realistic) femtocell configuration and argue that a co-tier avoidance scheme is indeed necessary to increase the performance of the femtocells. Path loss alone did not prove to give accurate estimate of level of co-tier interference. Fading and log-normal shadowing in addition to path loss provided accurate estimate of co-tier interference and also provided an accurate RoI for a femtocell. Our proposed novel resource allocation scheme reduces the interference probability from 90% to just 20%. Also the RB requirement probability was reduced

from 100% to just 33%.

The schemes proposed in this thesis can be implemented by a small modifications in the software and hardware in the femtocell base stations and in the femtocells UEs and in the macrocell UEs.

## 6.1 Future Work

In this thesis, schemes to avoid cross-tier and co-tier interference between femtocell networks were presented. Only DL interference scenarios were considered in this thesis. In future,

- Cross-tier UL interference scenarios in which the UL interference from MUE towards HNB and UL interference from HUE towards MNB will be considered.
- Co-tier UL interference scenarios in which UL interference from HUE towards a neighboring HNB will be considered.
- Fully self configured and self optimised femtocell architecture to avoid cross-tier and co-tier interference simultaneously inside a macrocell network will be considered.

Furthermore, a Pareto Optimal strategy will be implemented to allocate transmit power and resources in the femtocell and the macrocell network such that interference between the two networks can be avoided. Space time block coding will also be used to mitigate interference between femtocell and the macrocell. In space time block coding, multiple copies of the same transmitted signal is sent to the receiver through various antennas. The receiver re-constructs the transmitted signal from

the multiple copies received. Using space time block coding in the co-channel RB allocation environment can significantly lower the interference from undesired femto-cells. In addition, coherence theory methods to avoid interference in femtocells will be implemented to eliminate interference.

# Bibliography

- [1] V. Chandrasekhar, J. Andrews, and A. Gatherer, "Femtocell networks: a survey," *IEEE Commun. Mag.*, vol. 46, no. 9, pp. 59-67, Sep. 2008.
- [2] "Interference Management in UMTS femtocell," FemtoForum, Dec. 2008.[Online]: <http://www.scribd.com/doc/47418770/Interference-Management-in-UMTS-Femtocells>.
- [3] J. Chen, P. Rauber, D. Singh, C. Sundarramam, P. Tinnakornsriruphap, M. Yavuz, "Femtocells - Architecture and Network Aspects," Qualcomm, Jan. 2010. [Online]: <http://www.qualcomm.com/common/documents/white-papers/Femto-Overview-Rev-C.pdf>
- [4] V. Chandrasekhar, J. Andrews, "Spectrum Allocation in Tiered Cellular Networks," *IEEE Trans. Commun.*, vol. 57, no. 10, pp. 3059-3068, Oct, 2009.
- [5] V. Chandrasekhar, J. G. Andrews, "Spectrum Allocation in Two-Tier Networks," in *Proc. IEEE Asilomar Signals, Systems and Computers*, pp.1583,1587, 26-29 Oct. 2008

- [6] W. Yi, Z. Dongmei, J. Hai, W. Ye, "A Novel Spectrum Arrangement Scheme for Femtocell Deployment in LTE Macrocell," in *Proc. IEEE PIMRC*, pp. 6-11, 13-16 Sept, 2009.
- [7] N. Saquib, E. Hossain, L. B. Le and D. I. Kim, "Interference Management in OFDMA Femtocell Networks: Issues and Approaches," *IEEE Wireless Commun.*, vol. 19, no. 13, pp. 86-95, 2012.
- [8] DL Perez, A Valcarce, A Ladanyi, G De La Roche, J Zhang, "Intracell handover for interference and handover mitigation in OFDMA two-tier macrocell-femtocell networks," *EURASIP J Wirel Commun and Netw.*, 2010.
- [9] D. L. Perez, A. Valcarce, G. De La Roche, J. Zhang, " OFDMA Femtocells: A roadmap on interference avoidance," *IEEE Commun Mag.* vol. 47, no. 9, pp. 41-48, 2009.
- [10] M. Yavuz, F. Meshkati, S. Nanda, A. Pokhariyal, N. Johnson, B. Raghoehtaman, A. Richardson, " Interference Management and performace analysis of UMTS/HSPA+ Femtocells,". *IEEE Commun. Mag.*, vol. 47, no. 9, pp. 102-109, 2009.
- [11] 3GPP TR 25.820 V8.0.0, " Technical specification group radio access networks; 3G Home Node B study item technical report," March 2008.
- [12] 3GPP TR 25.968 V10.0.0, " Technical specification group radio access networks; 1.28Mcps TDD Home Node B radio frequency (RF)," Jan. 2011.

- [13] G. Gur, S. Bayhan, and F. Alagoz, "Cognitive femtocell networks: an overlay architecture for localized dynamic spectrum access [Dynamic Spectrum Management]," *IEEE Wireless Commun.*, vol. 17, no. 4, pp. 62-70, Aug. 2010.
- [14] J. Zhang, Ge. De. La Roche, *Femtocells: Technologies and Development*, A John Wiley&Sons, New York (2010).
- [15] European Cooperation in the Field of Scientific and Technical Research EURO-COST23 I, *Urban Transmission LOSS Models for Mobile Radio in the 900 and 1800 MHz Bands*, Revision 2, The Hague, September 1991.
- [16] E. Damosso, "Action COST 231: a commitment to the transition from GSM to UMTS ," *Personal Wireless Communications*, 1994., IEEE International Conference on , vol., no., pp.234-238, 18-19 Aug 1994.
- [17] J. Walfisch, and H. L. Bertoni, "A theoretical model of UHF propagation in urban environments," *IEEE Trans. Antennas and Propagation*, vol.36, no.12, pp.1788-1796, Dec 1988.
- [18] F. Pantisano, K. Ghaboosi, M. Bennis and M. Latva-Aho, "Interference avoidance via resource scheduling in TDD underlay femtocells," *IEEE PIMRC 2010*, vol., no., pp. 175-179. Sep. 2010.
- [19] J. Mitola III, "Cognitive radio: An integrated agent architecture for software defined radio," PhD Thesis, KTH Royal Institute of Technology, Sweden, May 2000.

- [20] Federal Communications Commission (FCC), “Facilitating opportunities for flexible, efficient, and reliable spectrum use employing cognitive radio technologies,” ET Docket No. 03-108, Mar. 2005.
- [21] Cognitive Radio Technology, [Online] Available: [http://www.ofcom.org.uk/research/technology/overview/emertech/cograd/cograd\\_main.pdf](http://www.ofcom.org.uk/research/technology/overview/emertech/cograd/cograd_main.pdf)
- [22] S. Haykin, “Cognitive radio: brain-empowered wireless communications,” *IEEE Journal on selected areas in communications*, vol. 23, no. 2, pp. 201-220, Feb. 2005.
- [23] IEEE Standard P1901.1/D01 (v 0.16), Standard Definitions and Concepts for Spectrum Management and Advanced Radio System Technologies (DRAFT), Jun. 2, 2006.
- [24] S. Srinivasa and S. A. Jafar, “The throughput potential of cognitive radio: A theoretical perspective,” *IEEE Commun. Mag.*, vol. 45, no. 5, pp. 73-79, May. 2007.
- [25] M. E. Sahin, I. Guvenc, J. Moo-Ryong, H. Arslan, “Handling CCI and ICI in OFDMA femtocell networks through frequency scheduling,” *IEEE Trans. Consumer Electronics*, vol.55, no.4, pp.1936-1944, Nov. 2009.
- [26] S.-M. Cheng, W. C. Ao, and C. K.-C. Chen, “Downlink capacity of two-tier cognitive femto networks,” *IEEE PIMRC 2010*, pp.1303-1308, 26-30 Sept. 2010.
- [27] I. Guvenc, J. Moo-Ryong, M. E. Sahin, X. Huilin, F. Watanabe, “Interference avoidance in 3GPP femtocell networks using resource partitioning and sensing,” in *Proc. IEEE PIMRC 2010*, pp.163-168, Sept. 2010

- [28] S. Barbarossa, S. Sardellitti, A. Carfagna, P. Vecchiarelli, "Decentralized interference management in femtocells: A game-theoretic approach," in *Proc. IEEE CROWNCOM 2010*, pp.1-5, 9-11 June 2010.
- [29] S.-Y. Lien and K.-C. Chen, Cognitive radio resource management for QoS guarantees in autonomous femtocell networks, in *Proc. IEEE ICC*, pp. 1-6, 23-27 May. 2010.
- [30] L. Yizhe, F. Zhiyong, Z. Qixun, T. Li, T. Fang, "Cognitive Optimization Scheme of Coverage for Femtocell Using Multi-Element Antenna," in *Proc. IEEE VTC 2010*, pp.1-5, Sept. 2010.
- [31] S. Nakwoon, J. P. M. Torregosa, H. Wonjoo, L. Sookjin, Y. Hyunsoo, "A joint power control and converge scheme in a cognitive-femtocell architecture for wireless networks for throughput maximization," in *Proc. IEEE INDIN 2010*, pp.1025-1030, July 2010.
- [32] S. Kaimaletu, R. Krishnan, S. Kalyani, N. Akhtar, and B. Ramamurthi, Cognitive interference management in heterogeneous femto-macro cell networks, *IEEE ICC*, pp. 16, June, 2011.
- [33] D.-C. Oh, H.-C. Lee, Y.-H. Lee, "Cognitive radio based femtocell resource allocation," *IEEE ICTC 2010*, pp.274-279, Nov. 2010.
- [34] M. Z. Chowdhury, R. Won, R. Eunjun, J. M. Yeong, "Handover between macro-cell and femtocell for UMTS based networks," in *Proc. IEEE ICACT 2009*, pp.237-241, Feb. 2009.

- [35] K. -S. Jin, L. -J. Tae, "Handover in UMTS networks with hybrid access femto-cells," in *Proc. IEEE ICACT 2010*, pp.904-908, Feb. 2010.
- [36] Z. Haijun, W. Xiangming, W. Bo, Z. Wei, S. Yong, "A Novel Handover Mechanism Between Femtocell and Macrocell for LTE Based Networks," in *Proc. IEEE ICCSN 2010*, pp.228-231, Feb. 2010.
- [37] U. Ardian, B. Robert, U. Melvi, "Handover Scenario and Procedure in LTE-based Femtocell Networks," in *Proc. UBICOMM 2010*, pp. 213-218, Oct. 2010.
- [38] W. -J. Shih, Lo. K. C. Steven, "Handover Scheme in LTE-based Networks with Hybrid Access Mode Femtocells," *Journal of Convergence Information Technology*, Vol. 6, no. 7, pp. 68-78, 2011.
- [39] Z. Becvar, P. Mach, "Adaptive Hysteresis Margin for Handover in Femtocell Networks," in *Proc. IEEE ICWMC 2010*, pp.256-261, Sept. 2010.
- [40] Z. Becvar, P. Mach, "Adaptive Hysteresis Margin for Handover in Femtocell Networks," in *Proc. ICN 2011*, pp.230-234, Jan. 2011.
- [41] Y.-Y. Li, M. Macuha, E. S. Sousa, T. Sato, and M. Nanri, "Cognitive interference management in 3G femtocells," in *Proc. PIMRC 2009*, pp.1118-1122, Sept. 2009.
- [42] Y.-Y Li, ES Sousa, Cognitive uplink interference management in 4G cellular femtocells, in *Proc. IEEE PIMRC*, pp. 1567-1571, Sept. 2010.
- [43] L. Zhang, L. Yang, T. Yang, "Cognitive interference management for LTE-A femtocells with distributed carrier selection," *IEEE VTC 2010*, pp. 1-5, Sept. 2010.

- [44] H. Li, X. Xu, D. Hu, X. Tao, P. Zhang, S. Ci, H. Tang, "Clustering strategy based on Graph method and power control for frequency resource management in femtocell and macrocell overlaid system," *Journal of Commun. and Netw.*, vol. 13, no. 6, pp. 664-677, Dec. 2011.
- [45] H. Widiarti, S. Pyun, and D. Cho, "Interference Mitigation Based on Femtocells Grouping in Low Duty Operation," in *Proc. IEEE VTC 2010*, pp. 15, Sept. 2010.
- [46] M. Husso, Z. Zheng, J. Hamalainen, E. Mutafungwa, "Dominant interferer mitigation in closed femtocell deployment," in *Proc. PIMRC 2010*, pp. 169-174, Sept. 2010.
- [47] M. Z. Chowdhury, J. M. Yeong, Z. J. Haas, "Interference mitigation using dynamic frequency re-use for dense femtocell network architectures," in *Proc. IEEE ICUFN 2010*, pp.256-261, June, 2010.
- [48] R. Berangi, **S. Saleem**, M. Faulkner and W. Ahmed, "TDD Cognitive Radio Femtocell Network (CRFN) Operation in FDD Downlink Spectrum," in *Proc. IEEE PIMRC 2011*, pp. 482-486, Sept. 2011.
- [49] R. G. Gallager, *Information Theory and Reliable Communication*. New York: Wiley, 1968.
- [50] T. M. Cover and J. A. Thomas, *Elements of Information Theory*. New York: Wiley, 1991.
- [51] W. Yu, and J. M. Cioffi, "On constant power water-filling," in *proc. ICC 2001*, vol.6, no., pp.1665-1669 vol.6, 2001.

- [52] D. P. Palomar, and J. R. Fonollosa, "Practical algorithms for a family of water-filling solutions," *IEEE Trans. Sig. Proc.*, vol. 53, no. 2, pp. 686- 695, Feb 2005.
- [53] P. K. Sharma and R. K. Singh, "Cell coverage area and link budget calculations in GSM system," *International Journal of Modern Engineering Research (IJMER)*, vol. 2, no. 2, pp. 170-176, Mar.-Apr.,2012.
- [54] Y. Tokgoz, F. Meshkati, Y. Zhou, M. Yavuz, S. Nanda, "Uplink interference management for HSPA+ and 1xEVDO femtocells," *IEEE GLOBECOM 2009*, pp. 1-7, Dec. 2009.
- [55] M. Matsumoto and T. Nishimura, "Mersenne Twister: A 623-dimensionally equidistributed uniform pseudorandom number generator," *ACM Transactions on Modeling and Computer Simulatio*, vol. 8, no. 1, pp. 330. 1998.
- [56] B. A. Forouzan, Data communications and networking. McGraw-Hill, 2007.
- [57] A. Rabbachin et al. "UWB energy detection in the presence of multiple narrow-band interferers," in *IEEE ICUWB 2007*, pp. 857 - 862, Sep. 2007.
- [58] A. Rabbachin et al. "Effect of aggregate narrowband interference on the UWB autocorrelation receiver," in *Proc. IEEE ICUWB 2008*, pp. 79-83, Sept. 2008.
- [59] **S. Saleem**, H. King, "Avoidance of Cross-tier Interference from Open Access Femtocells to Macrocell Users," *Jounral of Communication and Computer (JCC)*, pp. 929-941, vol. 9, no. 8, Aug. 2012.
- [60] M. Z. Win et al., "A mathematical theory of network interference and its applications," *Proceedings of the IEEE 2009*, vol. 97, no. 2, Feb. 2009.

- [61] M. S. Kim, H. W. Je, F. A. Tobagi, "Cross-tier interference mitigation for two tier OFDMA femtocell networks with limited macrocell information," in *Proc. IEEE Globecom*, pp. 1-5, 6-10 Dec. 2010.
- [62] **S. Saleem**, H. King, "Avoidance of Co-tier Interference between Femtocells with Different Access Modes," *International Journal of Information and Communication Technology Research (IJICTR)*, pp. 617-626, vol. 2, no. 8, Aug. 2012.